IN-02
380365
DATE OVERRIDE

TECHNICAL MEMORANDUM
X - 22

LIFT, DRAG, AND PITCHING MOMENTS OF AN ARROW WING

HAVING 80° OF SWEEPBACK AT MACH NUMBERS

FROM 2.48 TO 3.51 AND REYNOLDS NUMBERS

UP TO 11.0 MILLION

By Edward J. Hopkins, Don W. Jillie, and Alan D. Levin

Ames Research Center
Moffett Field, Calif.

NATIONAL AERONAUTICS AND SPACE ADMINISTRATION

NATIONAL AERONAUTICS AND SPACE ADMINISTRATION

TECHNICAL MEMORANDUM X-22

LIFT, DRAG, AND PITCHING MOMENTS OF AN ARROW WING

HAVING 80° OF SWEEPBACK AT MACH NUMBERS

FROM 2.48 TO 3.51 AND REYNOLDS NUMBERS

UP TO 11.0 MILLION*

By Edward J. Hopkins, Don W. Jillie, and Alan D. Levin

SUMMARY

Measurements were made of the lift, drag, and pitching moments on an arrow wing (taper ratio of zero) having an aspect ratio of 1.4 and a leading-edge sweepback of 80°. The wing was designed to have a subsonic leading-edge and a Clark-Y airfoil with a thickness ratio of 12 percent of the chord perpendicular to the wing leading edge. The wing was tested both with and without the wing tips bent upward in an attempt to alleviate possible flow separation in the vicinity of the wing tips. Small jets of air were used to fix transition near the wing leading edge. Force results are presented for Mach numbers of 2.48, 2.75, 3.04, 3.28, and 3.51 at Reynolds numbers of 3.5 and 9.0 million and for a Mach number of 3.04 at a Reynolds number of 11.0 million. The measured aerodynamic characteristics are compared with those estimated by linear theory. The maximum lift-drag ratio measured was much less than that predicted. This difference is attributed to lack of full leading-edge thrust and to the experimental lift-curve slope being about 20 percent below the theoretical value.

INTRODUCTION

An arrow wing having a subsonic leading edge and a sonic trailing edge can be shown theoretically to be an efficient wing with a high maximum lift-drag ratio at supersonic speeds (see refs. 1 and 2). Such a wing is shown in reference 1 to have less induced drag than either a triangular or rectangular wing with the same aspect ratio. An arrow wing designed for a Mach number of 3.0 has been investigated in the

Ames 1- by 3-foot supersonic wind tunnel at a Reynolds number of 3.5 million (ref. 3). At this Reynolds number visual-flow studies indicated flow separation along the wing leading edge.

The purpose of the present investigation of an arrow wing geometrically similar to that reported in reference 3 was to determine whether an increase in Reynolds number and air ejected through small orifices near the wing leading edge, in an attempt to fix transition, would alleviate flow separation.

NOTATION

C_D drag coefficient, $\dfrac{drag}{qS}$

C_L lift coefficient, $\dfrac{lift}{qS}$

C_m pitching-moment coefficient, $\dfrac{\text{pitching moment about } 0.35\bar{c}}{qS\bar{c}}$

C_{L_α} lift-curve slope measured at $\alpha = 0°$

$\dfrac{dC_m}{dC_L}$ pitching-moment curve slope measured at $\alpha = 0°$

$\dfrac{dC_D}{dC_L^2}$ drag-rise factor

C_{D_0} minimum drag coefficient

$\dfrac{L}{D}$ lift-drag ratio

b wing span

c' wing chord perpendicular to wing leading edge

$\bar{c}$ mean aerodynamic chord

L.E.   leading edge

M	Mach number
m	mass flow through the air-ejection orifices in the wing
q	free-stream dynamic pressure
R	Reynolds number based on the mean aerodynamic chord
S	wing area
α	angle of attack

APPARATUS AND MODEL DESCRIPTION

Wind Tunnel

The investigation was conducted in the 8- by 7-foot test section of the Ames Unitary Plan wind tunnel. The test-section Mach number can be set at any value from 2.4 to 3.5 during wind-tunnel operation by movement of the flexible nozzle walls. Total pressure can be maintained at any value from about 5 to 55 inches of mercury absolute. A more complete description of the wind tunnel is given in reference 4.

Model and Air Jets

The wing had 80° of sweepback at the leading edge, an aspect ratio of 1.4, and a taper ratio of zero. The ratio (volume)$^{2/3}$/(wing area) was 0.087. The airfoil perpendicular to the wing leading edge was the 12-percent-thick Clark-Y. A sketch of the wing plan form with pertinent dimensions is presented in figure 1(a). For part of the tests the wing tips were bent upward 3.72° about a lateral axis perpendicular to the plane of symmetry as shown in figure 1(a). This bend angle was made slightly larger than that used on the geometrically similar model tested in Ames 1- by 3-foot wind-tunnel, since the bend axis was necessarily more rearward in the present investigation. Both models were made of solid steel.

During part of the tests air was ejected through small orifices located at the chordwise stations shown in figure 1(b). Air was ejected at only one of these chordwise stations at a time.

Model Support

The model was supported on a sting which was attached to the lower surface of the wing as shown in figure 2. A six-component, electrical, strain-gage balance, located 34.85 inches behind the $0.35\bar{c}$ point, was used to measure the aerodynamic forces and moments. The balance and the sting were covered with a shroud which was tapered from about 6 inches in diameter in the vicinity of the balance to about 2.5 inches in width at the upstream end of the shroud to reduce the magnitude of the base drag correction.

TEST CONDITIONS AND TECHNIQUES

The tests were conducted at Mach numbers of 2.48, 2.75, 3.04, 3.28, and 3.51 at Reynolds numbers of 3.5 and 9.0 million. At a Mach number of 3.04 the model was also tested at a Reynolds number of 11.0 million. The angle of attack was varied from $-2°$ to $+6°$ in increments of $1°$.

Air ejection from either one of the two rows of orifices located near the wing leading edge was used as the boundary-layer trip since air jets produce a negligible wave drag, as indicated in reference 5. This method also has the advantage of controllability from outside the wind tunnel. The approximate mass flow required for fixing transition was estimated from reference 5 and from unpublished data taken during tests of a cone. During the force tests two mass flows were employed, one about equal to that estimated from reference 5 (about 0.008 slug/min) and one about twice that value. The flexible tube supplying air to the orifices was looped inside the shroud so that air flow through the tube would have a negligible effect on the balance measurements. With no air flow in the wind tunnel, variation of the air flow in the tube from zero to maximum flow was found to have a negligible effect on the balance forces.

Flow visualization techniques used to study the flow conditions in the boundary layer at a Mach number of 3.04 included the sublimation method of reference 6, the fluorescent-oil method, and the surface-tuft method. In the sublimation method fluorene was used as the subliming material and petroleum ether as the carrying agent. Oil-soluble fluorescent powder in oil was viewed under ultraviolet lights in the fluorescent-oil method.

CORRECTIONS AND ACCURACY

To obtain aerodynamic tares for the shrouded sting, measurements were made of the aerodynamic forces acting on the shrouded sting alone throughout the Mach number and Reynolds number ranges. These tares were subtracted from the data for the wing mounted on the sting to obtain final data for the wing alone. Although possible mutual interference effects between the model and the sting were neglected, these effects were estimated to be small.

Accuracy of the data based on the repeatability and known measuring precision of the instruments is as follows:

C_L	±0.002
C_m	±0.002
C_D	±0.0002
$(L/D)_{max}$	±0.3
α	±0.1°

The maximum Mach number variation in the wind tunnel in the vicinity of the model was ±0.05. The Mach numbers shown in the figures were those at the position of the leading edge of the mean aerodynamic chord in the empty test section.

THEORETICAL METHODS OF ANALYSIS

The lift and pitching-moment curve slopes were calculated by the method of reference 2. The drag-rise factor, dC_D/dC_L^2, the full leading-edge thrust, was also calculated by this method. For the case of no leading-edge thrust the drag due to lift was assumed to be equal to the lift times the angle of attack. The wave-drag portion of the minimum drag was estimated by the method of reference 7. In these wave-drag calculations the airfoil was assumed to have the same distribution of area as the Clark-Y airfoil perpendicular to the wing leading edge but was assumed to be symmetrical about its chord line. Such an assumption is justified since the airfoil had a maximum thickness of only 3.2 percent of the chord in the stream direction. To estimate the skin-friction drag portion of the minimum drag it was, of course, necessary to know the chordwise location of boundary-layer transition. The approximate transition location was measured at various stations along the wing span on

the sublimation photographs taken at a Mach number of 3.04. The method of reference 8, with the compressibility factors from references 9 and 10 for the turbulent and laminar boundary layers, was used to estimate the skin-friction drag coefficients. In the estimates no account was taken of possible transition movement due to Mach number changes. This assumption seemed justified since unpublished transition data taken on a cone at a constant Reynolds number in the same wind tunnel indicated a negligible transition movement over the same Mach number range as for the present tests.

RESULTS AND DISCUSSION

Presentation of Results

The lift, drag, pitching-moment, and lift-drag ratio results are presented in figures 3 to 9, inclusive. Reynolds numbers, Mach numbers, and air-ejection conditions with the corresponding figure numbers are given in the following table.

Mach no.	$R \times 10^{-6}$	Air ejection	Wing tip	Figure
2.48, 2.75, 3.04, 3.28, 3.51	3.5, 9.0	Off	Unbent	3
2.48, 2.75, 3.04, 3.28, 3.51	3.5, 9.0	At 0.05c'	Unbent	4
3.04, 3.28, 3.51	3.5, 9.0	At L.E.	Unbent	5
3.04	11.0	Off, at L.E. and at 0.05c'	Unbent	6
2.48, 2.75, 3.04, 3.28, 3.51	3.5, 9.0	Off	Bent	7
2.48, 2.75, 3.04, 3.28, 3.51	3.5, 9.0	At L.E.	Bent	8
3.04	11.0	Off and at L.E.	Bent	9

The lift and pitching-moment curve slopes, the maximum lift-drag ratios, the minimum drag coefficients, the lift coefficients at $(L/D)_{max}$, and the drag-rise factors taken from the data of figures 3 to 8 are summarized in figure 10. A single curve is presented for the lift-curve slope for the different flow conditions at a given Mach number because any measurable differences were within the estimated accuracy of the data.

Results from reference 3 for a smaller but geometrically similar wing at a Reynolds number of 3.5 million and a Mach number of 3.0 are included in figure 10. Theoretical results, which are discussed later in the report, are also shown for comparison.

Discussion of Experimental Results

Wing flow conditions.- Studies of the flow conditions on the wing were made to establish the extent of flow separation and the location of boundary-layer transition. On the geometrically similar wing, reported upon in reference 3, white-lead studies indicated flow separation along the wing leading edge. In the present tests, at a Mach number of 3.04, tuft and fluorescent-oil studies showed evidence of boundary-layer flow in the direction of the wing tip. This spanwise flow appeared progressively closer to the wing leading edge as the angle of attack was increased from 0° to 6°. Although there was no evidence of flow separation along the entire wing leading edge, some evidence of a vortex-type flow existing above the upper surface of the wing was particularly discernible in the tuft and sublimation studies. At an angle of attack of 0°, on the inboard half of the wing span, the subliming film indicated that transition occurred between the wing leading edge and the 15-percent chord line at a Reynolds number of 11.0 million and between the 20- and 30-percent chord lines at a Reynolds number of 3.5 million. On the outboard half of the wing span, transition appeared to occur near the wing leading edge at a Reynolds number of 11.0 million and at about the 50-percent chord line at a Reynolds number of 3.5 million. Air ejection at the leading edge moved transition forward as much as 15 percent of the wing chord at a Reynolds number of 3.5 million and in some local areas up to the wing leading edge at a Reynolds number of 11.0 million.

Force coefficients (unbent wing tips).- With no air ejection an increase in Reynolds number from 3.5 to 9.0 million had a negligible effect on the aerodynamic characteristics (see fig. 3). A further increase in Reynolds number to 11.0 million at a Mach number of 3.04 also caused a negligible change in any of the coefficients (see fig. 6). Evidently, the reduction in skin-friction drag due to an increase in Reynolds number was approximately canceled by the additional skin-friction drag associated with the slightly larger turbulent boundary-layer areas observed in the sublimation studies. At a Reynolds number of 3.5 million, air ejection[1] at the 5-percent chord line gave a small increase in the minimum drag coefficient, probably as a result of the increased skin-friction drag associated with a forward movement of transition, and resulted in a decrease of the maximum lift-drag ratio (see figs. 10(b) and 10(c)). A much smaller decrease due to air ejection was measured

[1]Data for only one ejection flow rate are presented, since doubling the ejection flow rate produced a negligible change in the force data.

at the Reynolds number of 9.0 million than at 3.5 million probably because transition was already near the leading edge as indicated by the sublimation studies. At either a Reynolds number of 3.5 or 9.0 million air ejection at the wing leading edge produced no change in the minimum drag coefficient or the maximum lift-drag ratio as shown in figures 10(b) and 10(c).

Force coefficients (bent wing tips).- In an attempt to relieve any possible flow separation and to trim at the lift coefficient for maximum lift-drag ratio, the wing tips were bent upward as indicated under APPARATUS AND MODEL DESCRIPTION. Comparison of figures 7(b) and 10(c) shows that trim occurred considerably below the C_L for $(L/D)_{max}$ which differs with the data of reference 3 in which trim occurred approximately at C_L for $(L/D)_{max}$. This difference might be attributed to differences in aeroelastic effects since the dynamic pressure acting on the model of reference 3 was eight times the dynamic pressure acting on the model used in the present investigation at the same Reynolds number. The wing-tip bend gave an appreciable increase in the maximum lift-drag ratio at a Reynolds number of 3.5 million but a small change in this ratio at a Reynolds number of 9.0 million throughout the Mach number range (fig. 10(c)). In general, air ejection at the wing leading edge reduced considerably the maximum lift-drag ratio at a Reynolds number of 3.5 million but caused a very small decrease in this ratio at a Reynolds number of 9.0 million. For either Reynolds number, at all air-ejection conditions, bending the wing tips gave a slight increase in the minimum drag coefficients (fig. 10(b)) and a decrease in the drag-rise factor (fig. 10(d)).

Summary of the maximum lift-drag ratios.- To assist in the evaluation of the efficiency of the arrow wing at a Mach number of 3.04 at the various test conditions the maximum lift-drag ratios obtained from figures 6, 9, and 10 are summarized below.

Wing tips	Air ejection	$R \times 10^{-6}$	$(L/D)_{max}$	Wing tips	Air ejection	$R \times 10^{-6}$	$(L/D)_{max}$
Unbent	Off	3.5	8.5	Unbent	At 0.05c'	9.0	8.2
Unbent	Off	9.0	8.5	Unbent	At L.E.	9.0	8.5
Unbent	Off	11.0	8.6	Unbent	At 0.05c'	11.0	8.3
Bent	Off	3.5	9.4	Unbent	At L.E.	11.0	8.6
Bent	Off	9.0	8.6	Bent	At L.E.	3.5	8.9
Bent	Off	11.0	8.7	Bent	At L.E.	9.0	8.6
Unbent	At 0.05c'	3.5	7.7	Bent	At L.E.	11.0	8.7
Unbent	At L.E.	3.5	8.5				

Comparisons in the above table indicate that without air ejection and with unbent tips, an increase in Reynolds number from 3.5 to 11.0 million increased $(L/D)_{max}$ only from 8.5 to 8.6. Bending the wing tips at a

Reynolds number of 3.5 million with no air ejection increased $(L/D)_{max}$ from 8.5 to 9.4, but at a Reynolds number of 11.0 million increased $(L/D)_{max}$ only from 8.6 to 8.7 either with or without air ejection at the leading edge. Part of the difference in the effects on $(L/D)_{max}$ of bending the wing tips at these two Reynolds numbers can be attributed to the fact that a smaller increase in the minimum drag due to bending was measured at a Reynolds number of 3.5 million than at a Reynolds number of 11.0 million. Compare figures 6, 9, and 10.

Comparison Between Experiment and Theory

The estimated lift-curve slopes were considerably higher than the experimental values (fig. 10(a)). This difference might be partly attributed to the drain of the boundary layer near the wing trailing edge at the inboard span stations to the wing tip which was not considered in the estimated values. This effect would produce an effective negative camber and thereby reduce the lift-curve slope as suggested in reference 11. The estimated forward movement of the aerodynamic-center location for Mach numbers at which the trailing edge was subsonic does not show up in the experimental measurements (fig. 10(a)), probably because a large portion of the trailing edge was in effect subsonic at all times as a result of the Mach cone from the balance shroud. Predicted variation of the minimum drag coefficient with Mach number shows good agreement with the experimental variation, but the estimated values were about 0.0005 higher than the experimental values at a Reynolds number of 9.0 million (fig. 10(b)). The maximum lift-drag ratio was estimated to be considerably higher than the experimental value (fig. 10(c)), probably because full leading-edge thrust was not realized and the lift-curve slope was lower than estimated. For example, at a Mach number of 3.0 and a Reynolds number of 9.0 million for the wing with no air ejection, the theoretical values of maximum lift-drag ratios were about 12.2 and 9.2 with and without leading-edge thrust, respectively, as compared with a measured value of about 8.5. This result is substantiated in figure 10(d) in which at a Mach number of 3.0 the measured drag-rise factor is 0.92 as compared with the theoretical value of 0.87 for no leading-edge thrust. The fact that the experimental maximum lift-drag ratio is not even as high as the predicted value for no leading-edge thrust as shown in figure 10(c) can be explained by the estimated lift-curve slope being about 20 percent above the experimental value. The amount of leading-edge thrust which was realized can be estimated from the drag-rise equation below:

$$\frac{dC_D}{dC_L{}^2} = \frac{1}{57.3C_{L_\alpha}} - K_T \tag{1}$$

where K_T is the thrust constant and C_{L_α} is the lift-curve slope per degree. At a Mach number of 3.0 the theoretical value of K_T is 0.50. If the measured values for the lift-curve slope (0.016) and the drag-rise factors (0.82 with bent tip and 0.92 without bent tips) are used in equation (1), then K_T equals 0.29 and 0.17 for the wing with and without the wing-tip bend, respectively. Thus an increase in leading-edge thrust was realized by bending the wing tips upward but the measured values are well below the theoretical value.

CONCLUDING REMARKS

Results of an investigation of an arrow wing having an aspect ratio of 1.4 and a leading-edge sweepback of 80° at Reynolds numbers from 3.5 to 11.0 million throughout a Mach number range from 2.48 to 3.51 indicate that a Reynolds number increase from 3.5 to 11.0 million did not increase the maximum lift-drag ratio for the wing with the unbent tips. Bending the wing tips upward increased the maximum lift-drag ratio from about 8.5 to 9.5 at a Reynolds number of 3.5 million, but did not increase this ratio at a Reynolds number of 11.0 million. Air ejection at the wing leading edge had no effect on the maximum lift-drag ratio at Reynolds numbers of 9.0 or 11.0 million. The maximum lift-drag ratio predicted by linear theory for the wing was much larger than that measured. The difference between the experimental and theoretical lift-drag ratios was attributed to lack of full leading-edge thrust and to the experimental lift-curve slope being about 20 percent below the theoretical value. It is possible that the effect of the boundary-layer flow in the direction of the wing tip near the wing trailing edge, indicated by the visual-flow studies, can account for the difference in the experimental and theoretical lift-curve slopes.

Ames Research Center
    National Aeronautics and Space Administration
        Moffett Field, Calif., March 13, 1959

REFERENCES

1. Beane, B. J.: Curves of Minimum Wave Plus Vortex Drag Coefficient for Several Wing Planforms. Douglas Rep. SM-22989, Nov. 1957.

2. Cohen, Doris: Formulas for the Supersonic Loading, Lift, and Drag of Flat Swept-Back Wing With Leading Edges Behind the Mach Lines. NACA Rep. 1050, 1951.

3. Katzen, Elliott D.: Idealized Wings and Wing-Bodies at a Mach
       Number of 3. NACA TN 4361, 1958.

4. Huntsberger, Ralph F., and Parsons, John F.: The Design of Large
       High-Speed Wind Tunnels. AGARD Rep. AG 15/P6, May 1954.

5. Coles, Donald: Measurements in the Boundary Layer on a Smooth Flat
       Plate in Supersonic Flow. III. Measurement in a Flat-Plate
       Boundary Layer at the Jet Propulsion Laboratory. Rep. 20-71,
       Jet Propulsion Laboratory, CIT, June 1, 1953.

6. Main-Smith, J. D.: Chemical Solids as Diffusible Coating Films for
       Visual Indications of Boundary-Layer Transition in Air and Water.
       British Rep. Chem. 466, 1950. (Also available as R. & M. No. 2755,
       British)

7. Holdaway, George H., and Hatfield, Elaine W.: Investigation of
       Symmetrical Body Indentations Designed to Reduce the Transonic
       Zero-Lift Wave Drag of a 45° Swept Wing With an NACA 64A006 Section
       and With a Thickened Leading-Edge Section. NACA RM A56K26, 1957.

8. Hall, Charles F., and Fitzgerald, Fred F.: An Approximate Method
       For Calculating the Effect of Surface Roughness on the Drag of an
       Airplane. NACA RM A7B24, 1947.

9. Reshotko, Eli, and Tucker, Maurice: Approximate Calculation of the
       Compressible Turbulent Boundary Layer With Heat Transfer and Arbi-
       trary Pressure Gradient. NACA TN 4154, 1957.

10. Van Driest, E. R.: Investigation of Laminar Boundary Layer in
       Compressible Fluids Using the Crocco Method. NACA TN 2597, 1952.

11. Preston, J. H.: The Calculation of Lift Taking Account of the
       Boundary Layer. R. & M. No. 2725, British A.R.C., 1953.
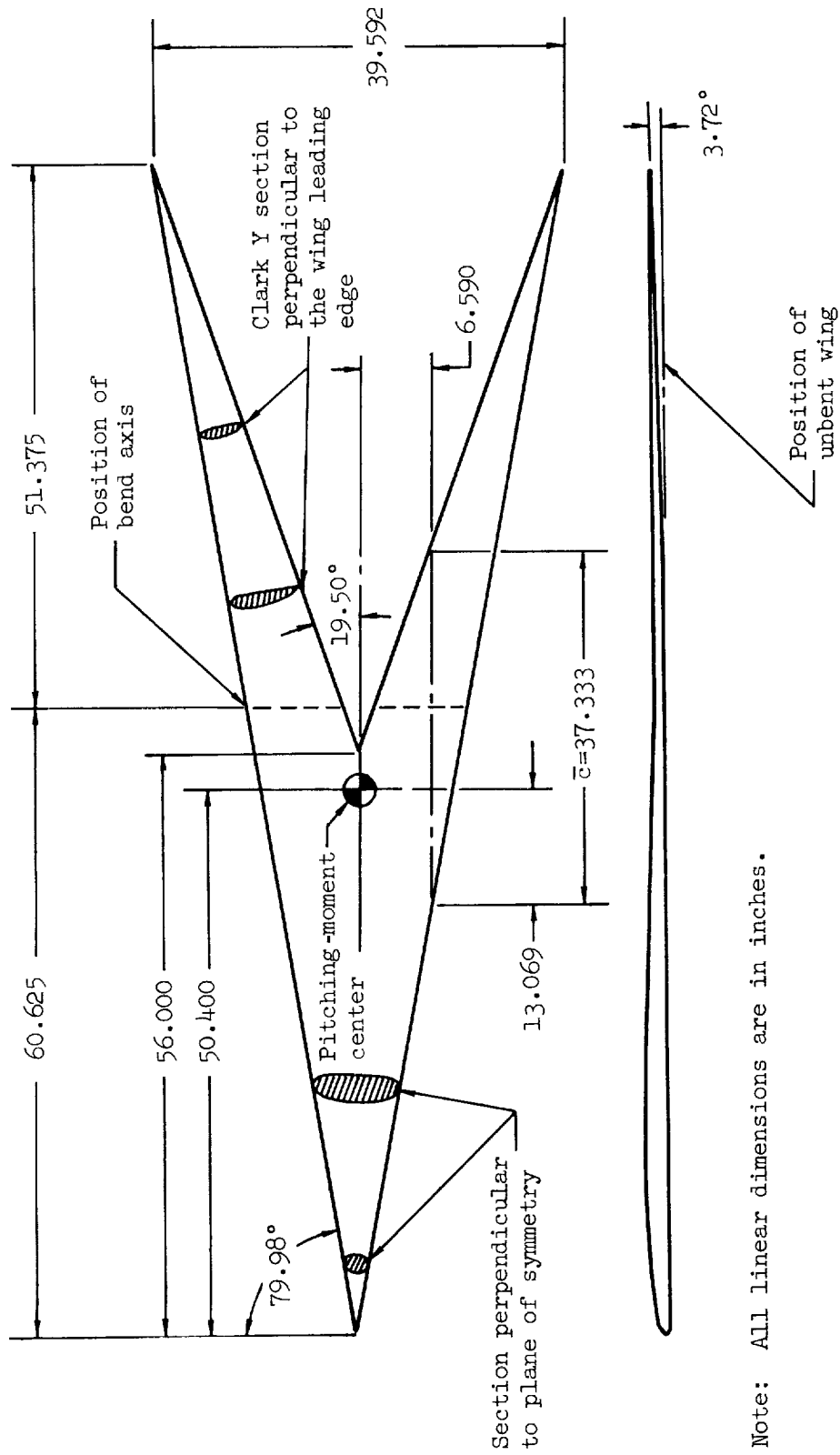
Figure 1.- Arrow wing dimensions and orifice locations.

(a) Plan-form dimensions.

Note: All linear dimensions are in inches.

0.75 of L.E.

Orifices spaced $\frac{1}{4}$" apart along
this portion of each wing panel

0.05 of L.E.

A

A

0.05c'

Manifolds

Orifices at leading edge
and 0.05c', 0.0135 inch
in diameter

Section A-A

Typical location of orifices
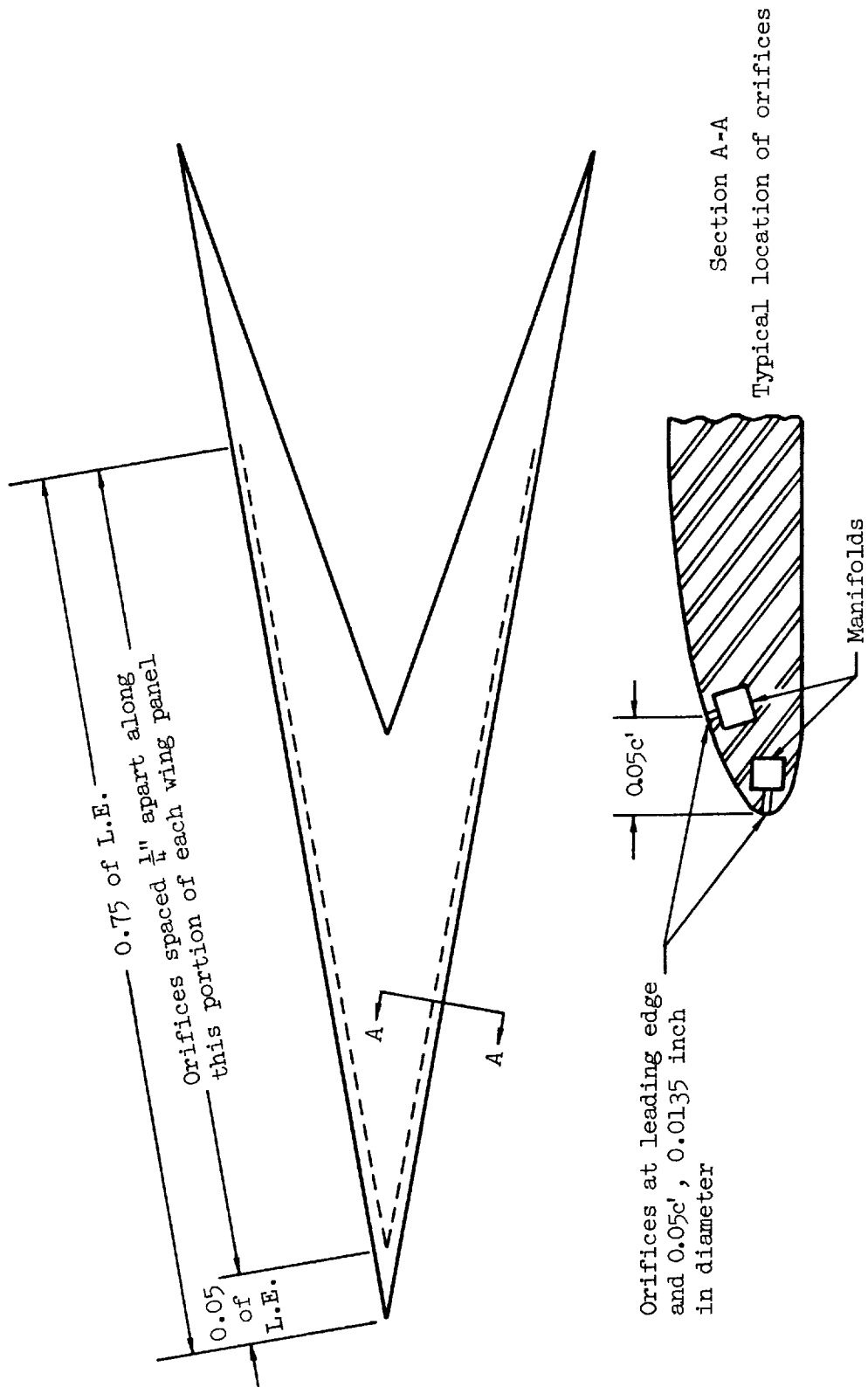
(b) Orifice locations.

Figure 1.- Concluded.

Figure 2.- Arrow wing with bent wing tips mounted in the Ames 8- by 7-foot wind tunnel.
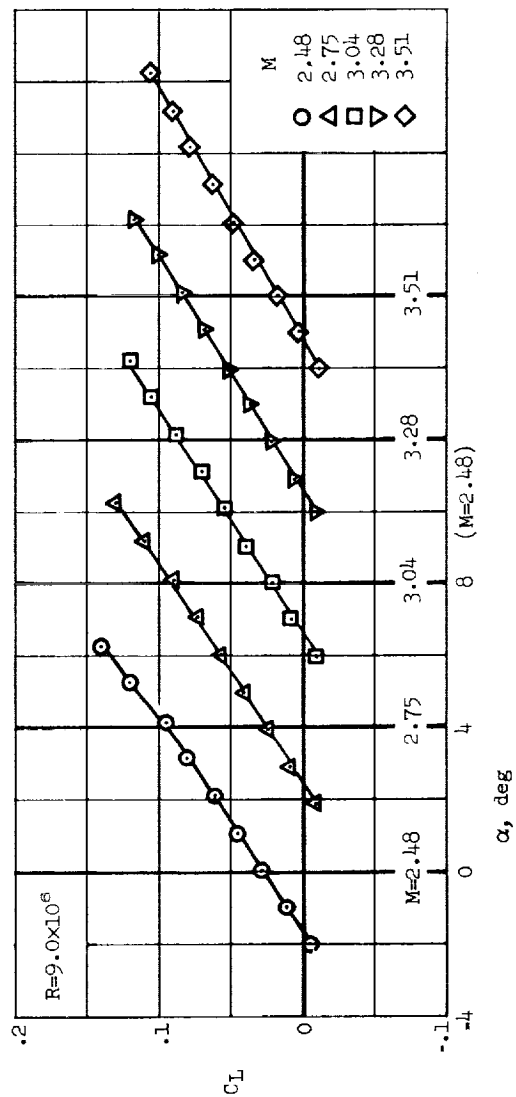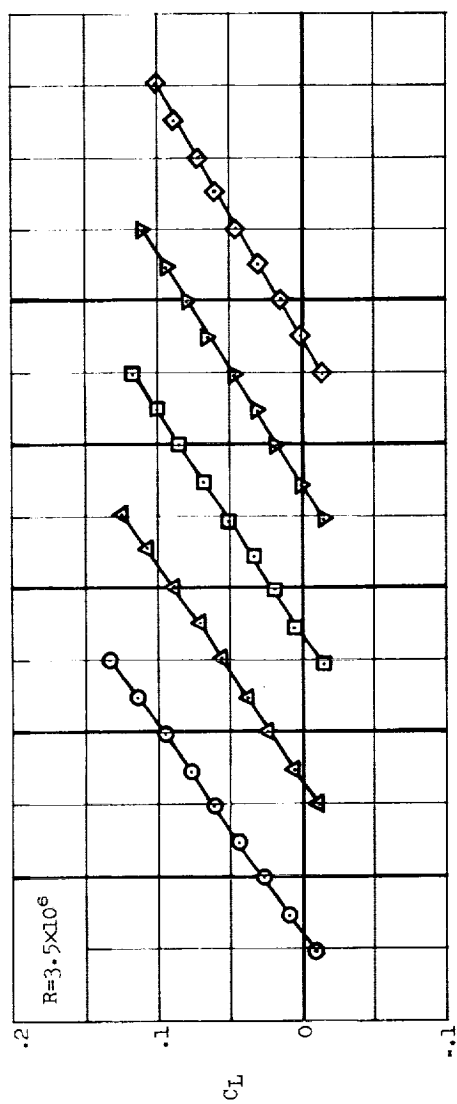
(a) C_L vs. α

Figure 3.- Lift-drag, pitching-moment, and lift-to-drag ratio characteristics for the arrow wing with the unbent wing tips. No air ejection.
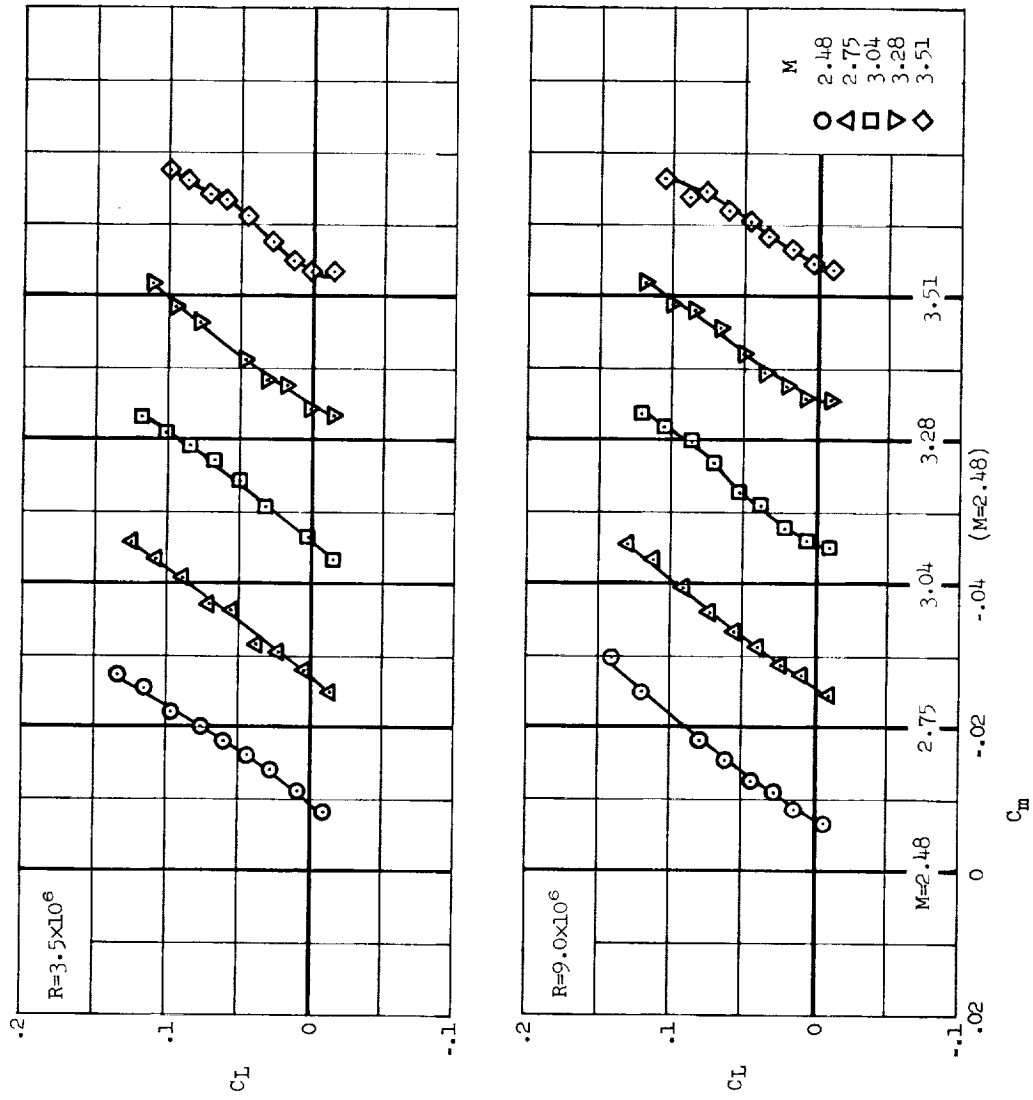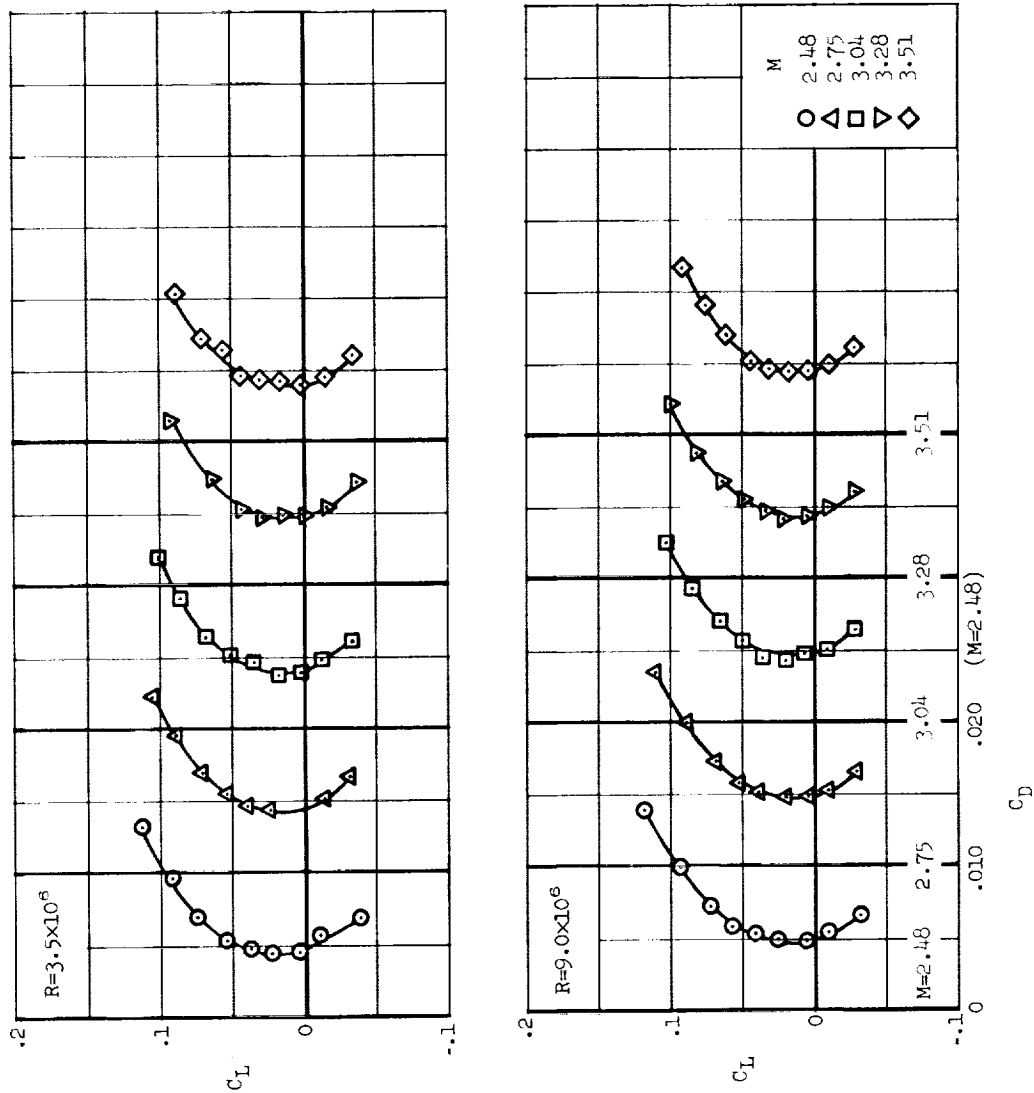
(b) C_L vs. C_m

Figure 3.- Continued.
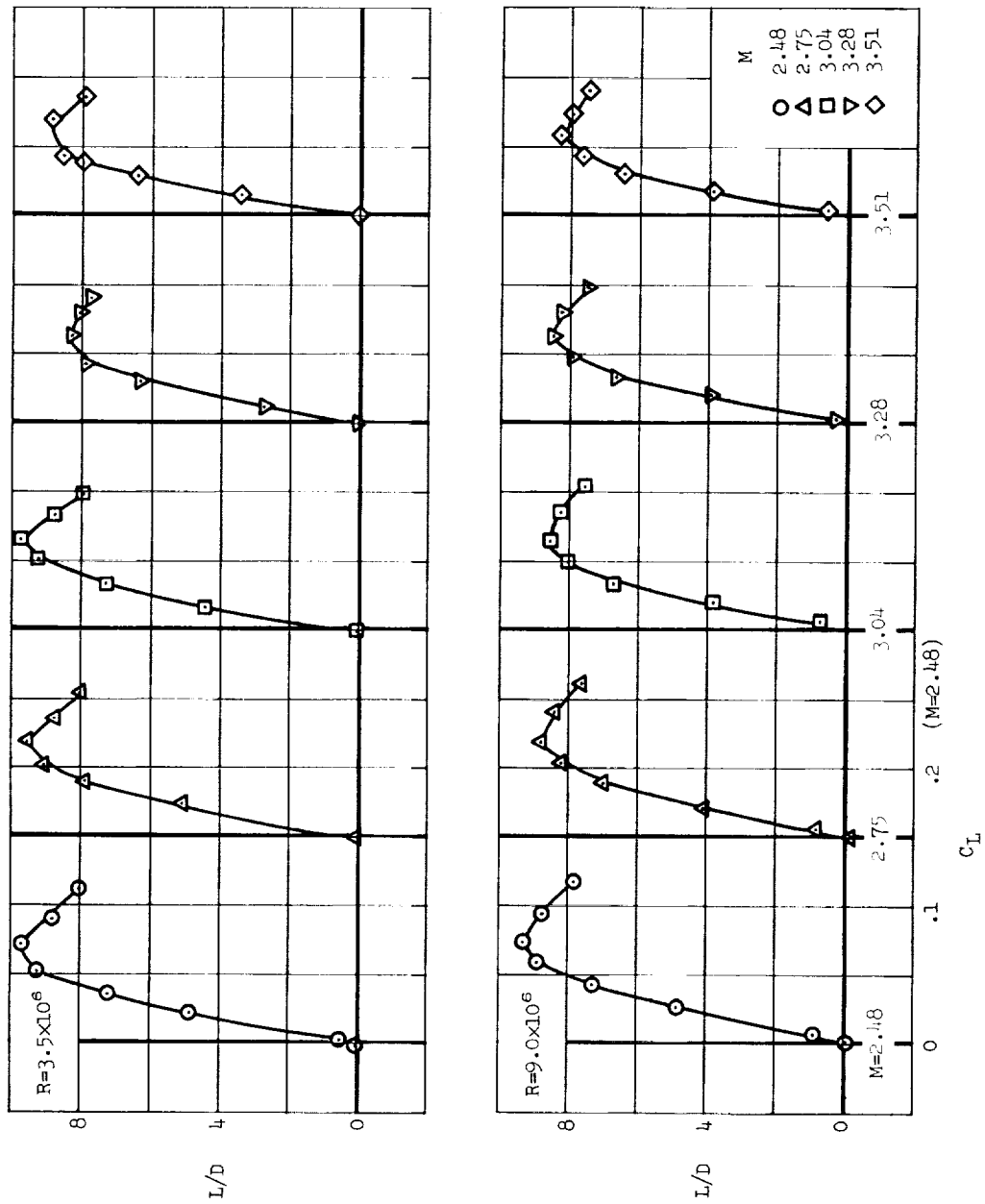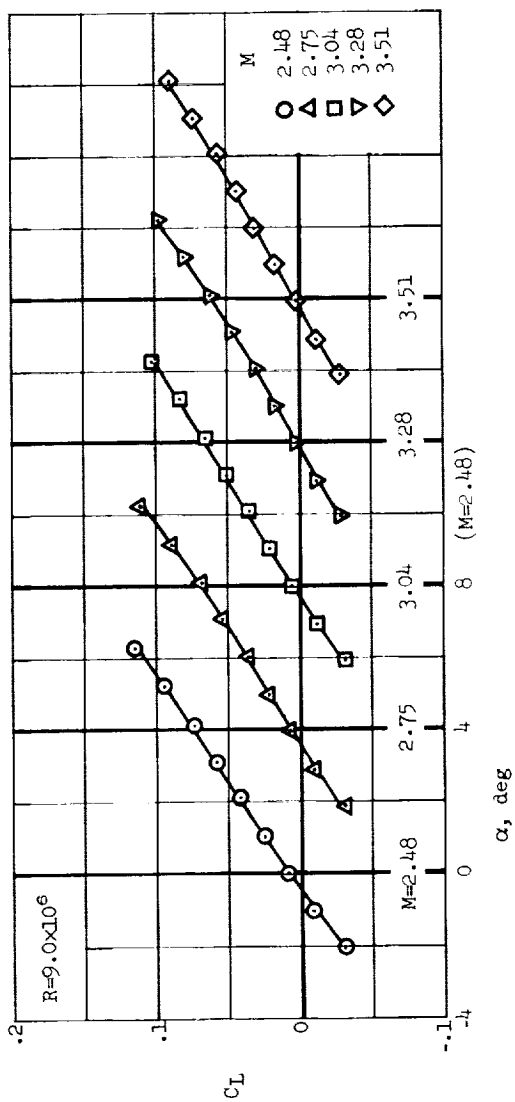
18
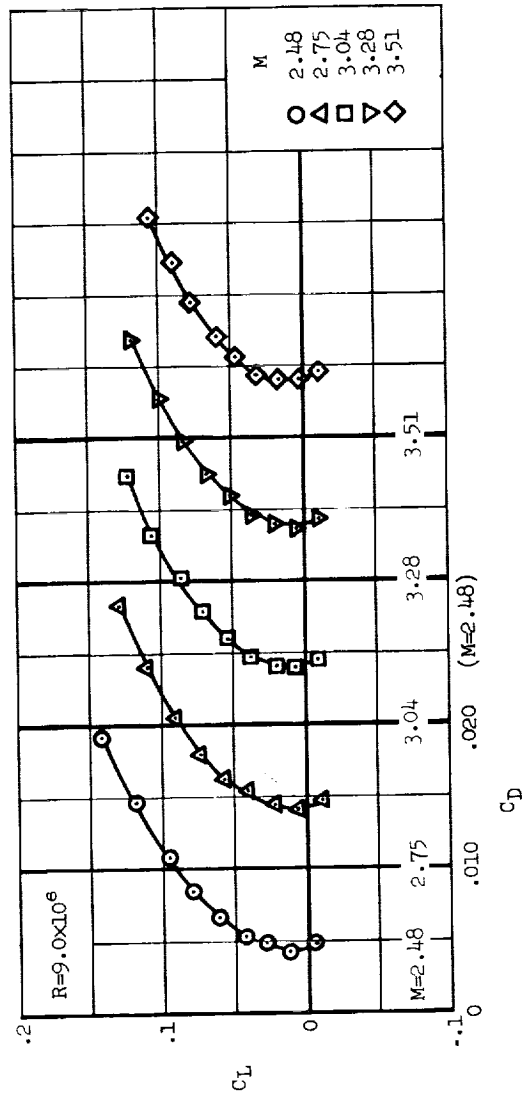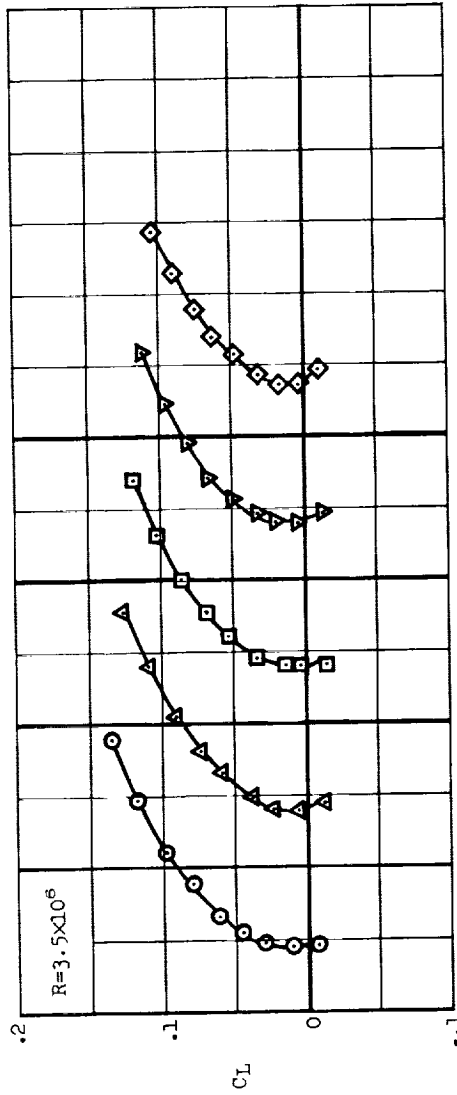
(c) C_L vs. C_D
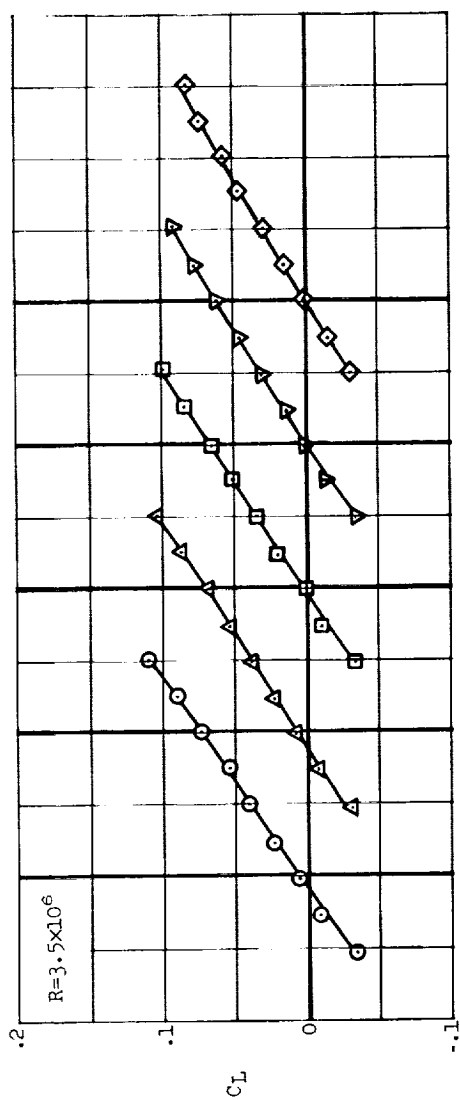
Figure 3.- Continued.
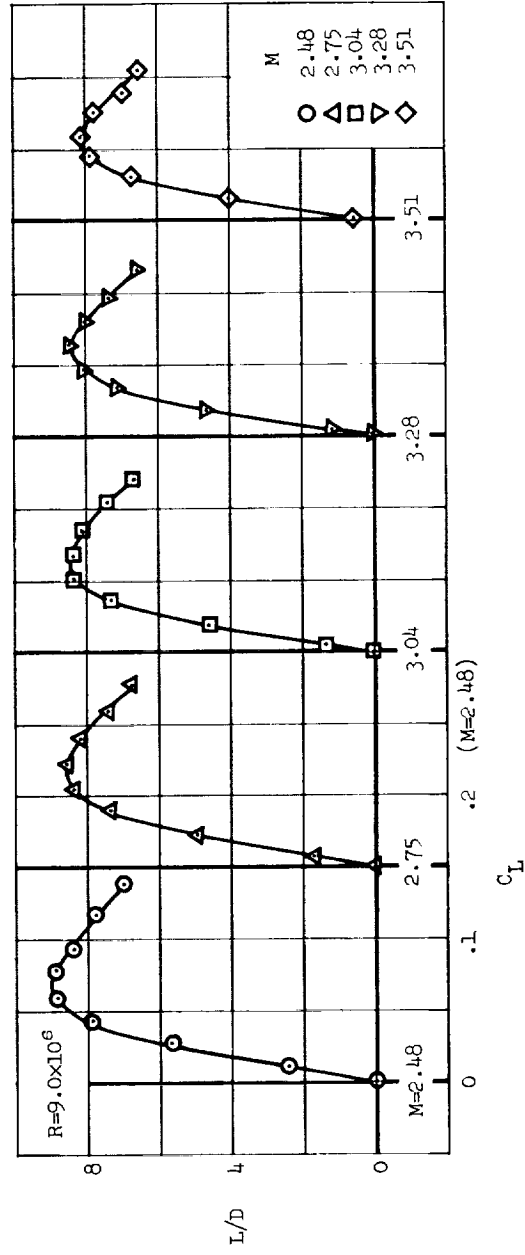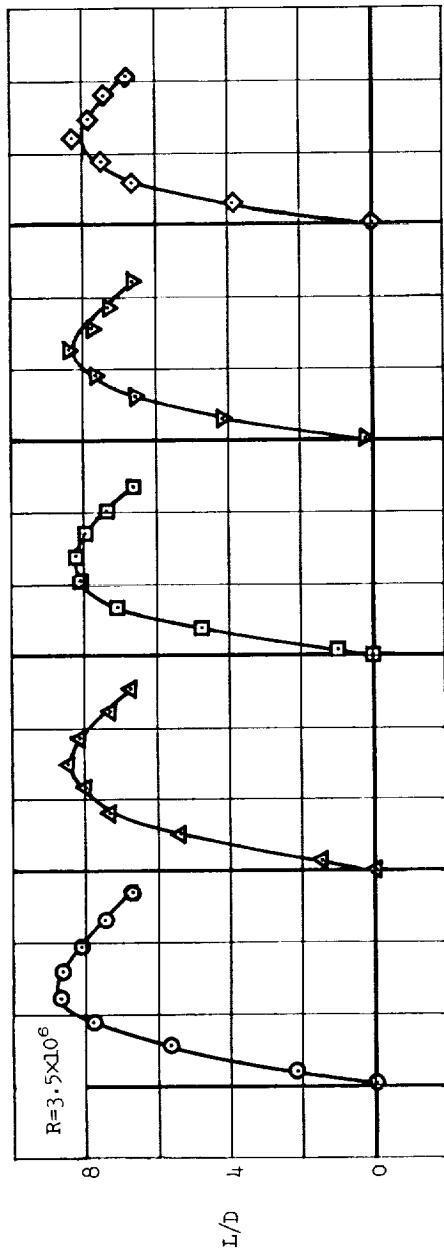
(d) L/D vs. c_L

Figure 3.— Concluded.
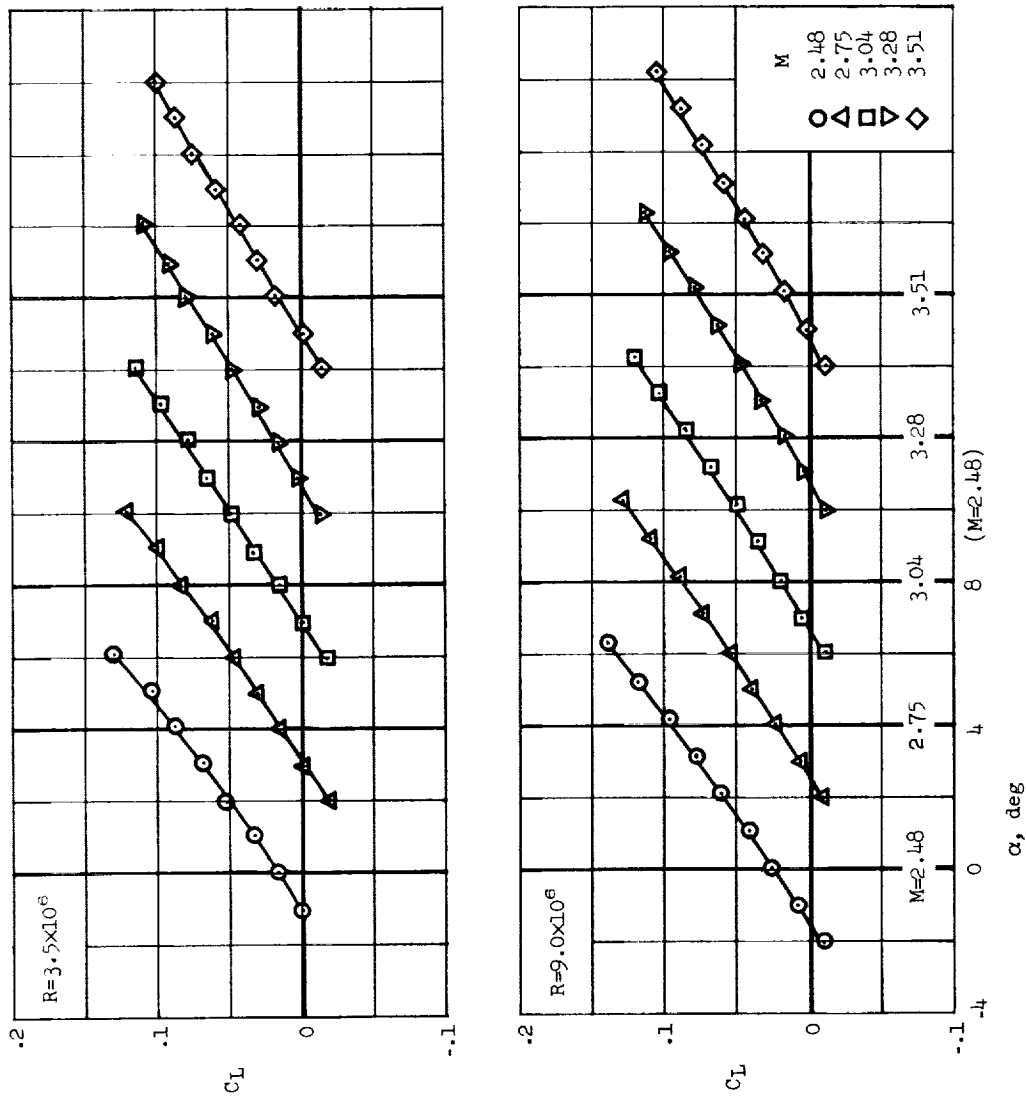
(a) C_L vs. α

Figure 4.- Lift, drag, pitching-moment, and lift-to-drag ratio characteristics for the arrow wing with the unbent wing tips; air ejected at 0.05c'; m=0.008 slugs/min.
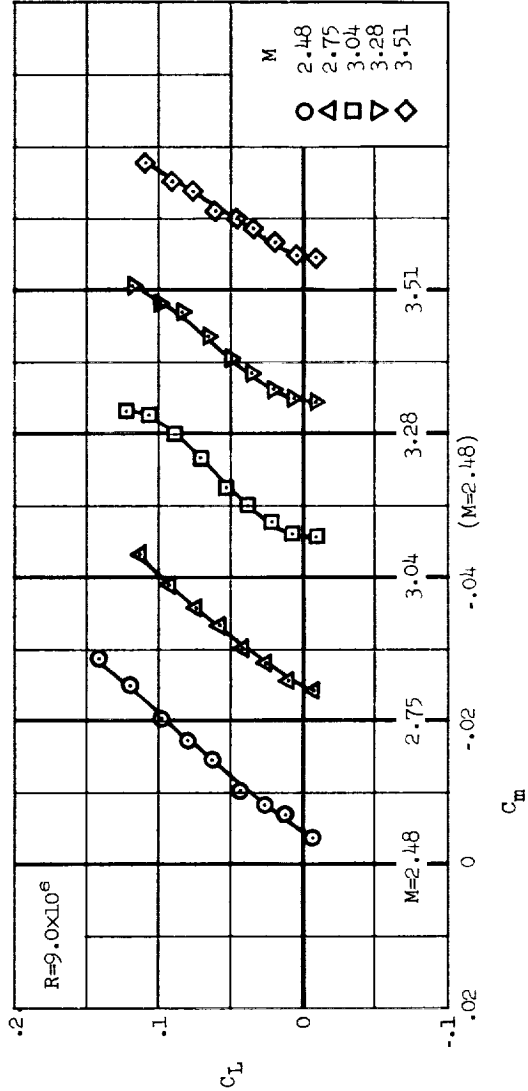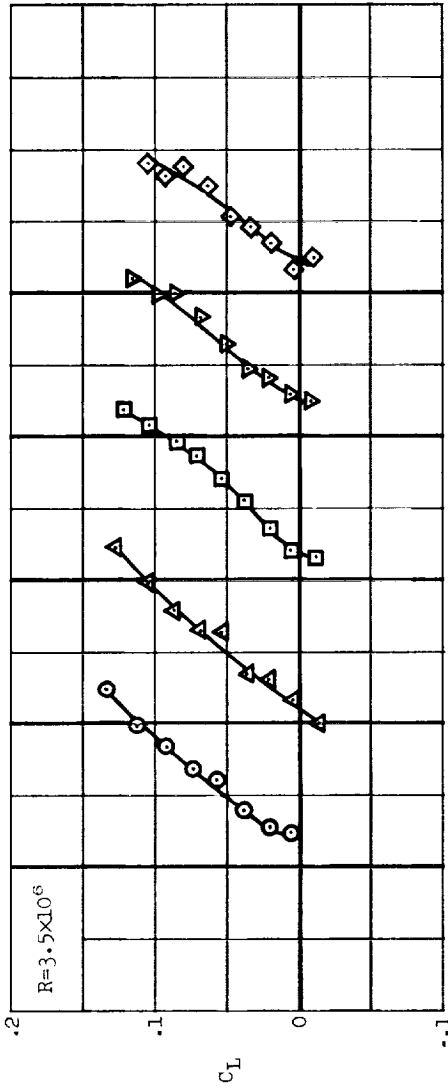
(b) C_L vs. C_m

Figure 4.- Continued.
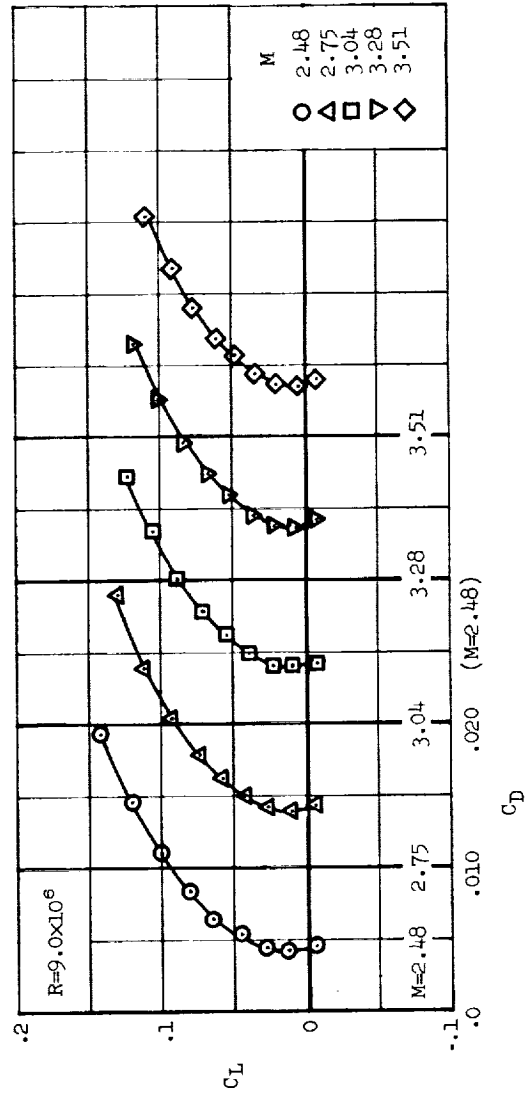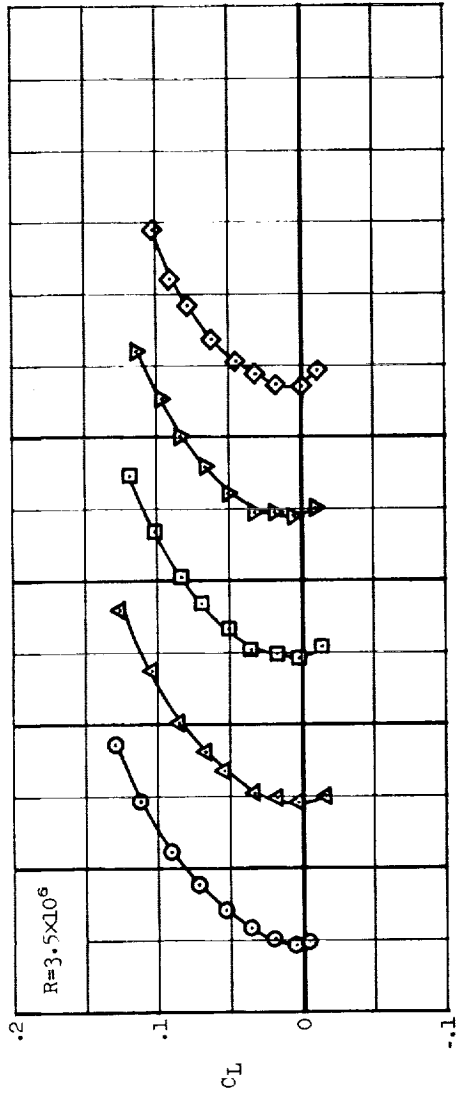
(c) C_L vs. C_D

Figure 4. - Continued.
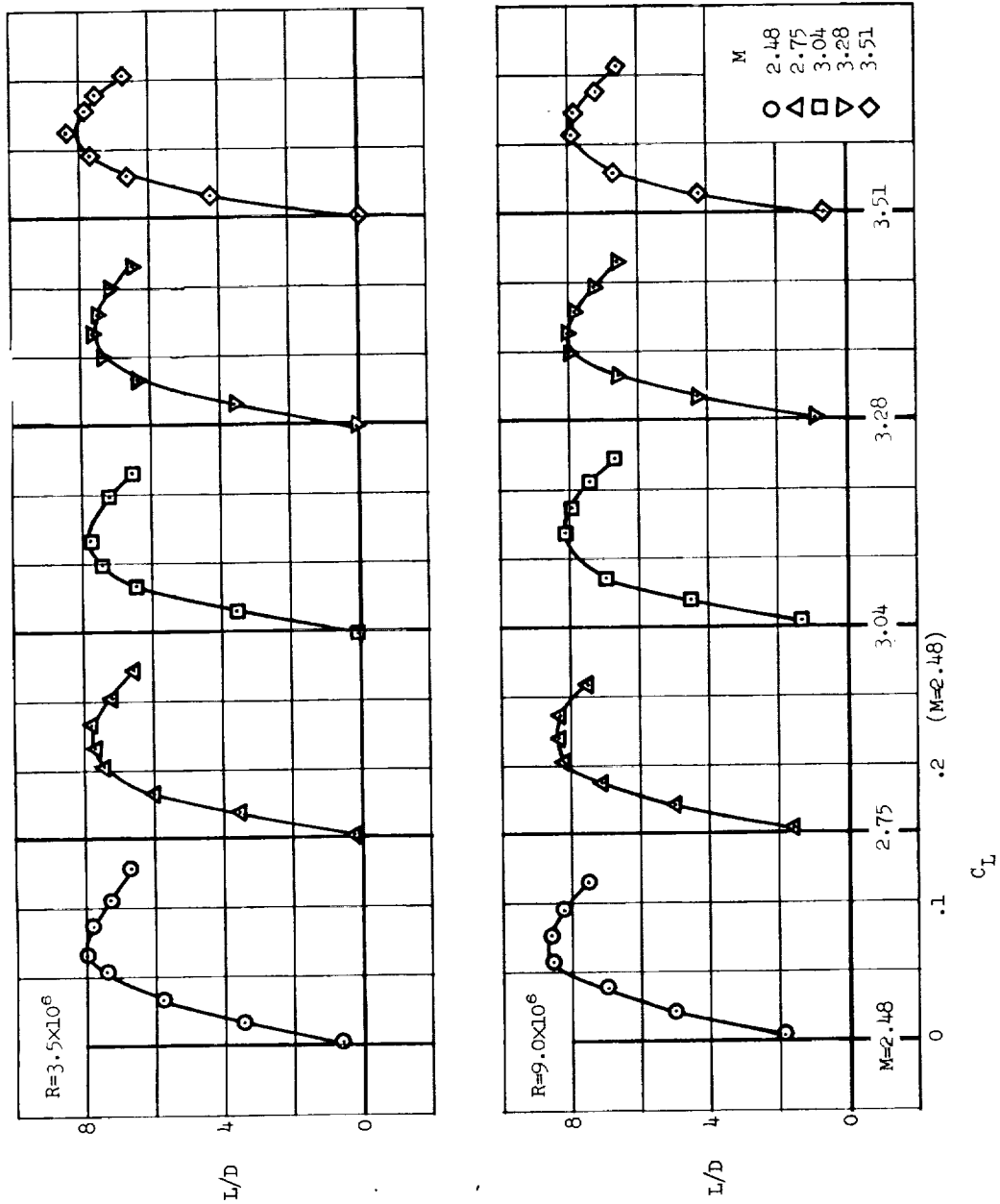
(d) L/D vs. C_L

Figure 4.- Concluded.
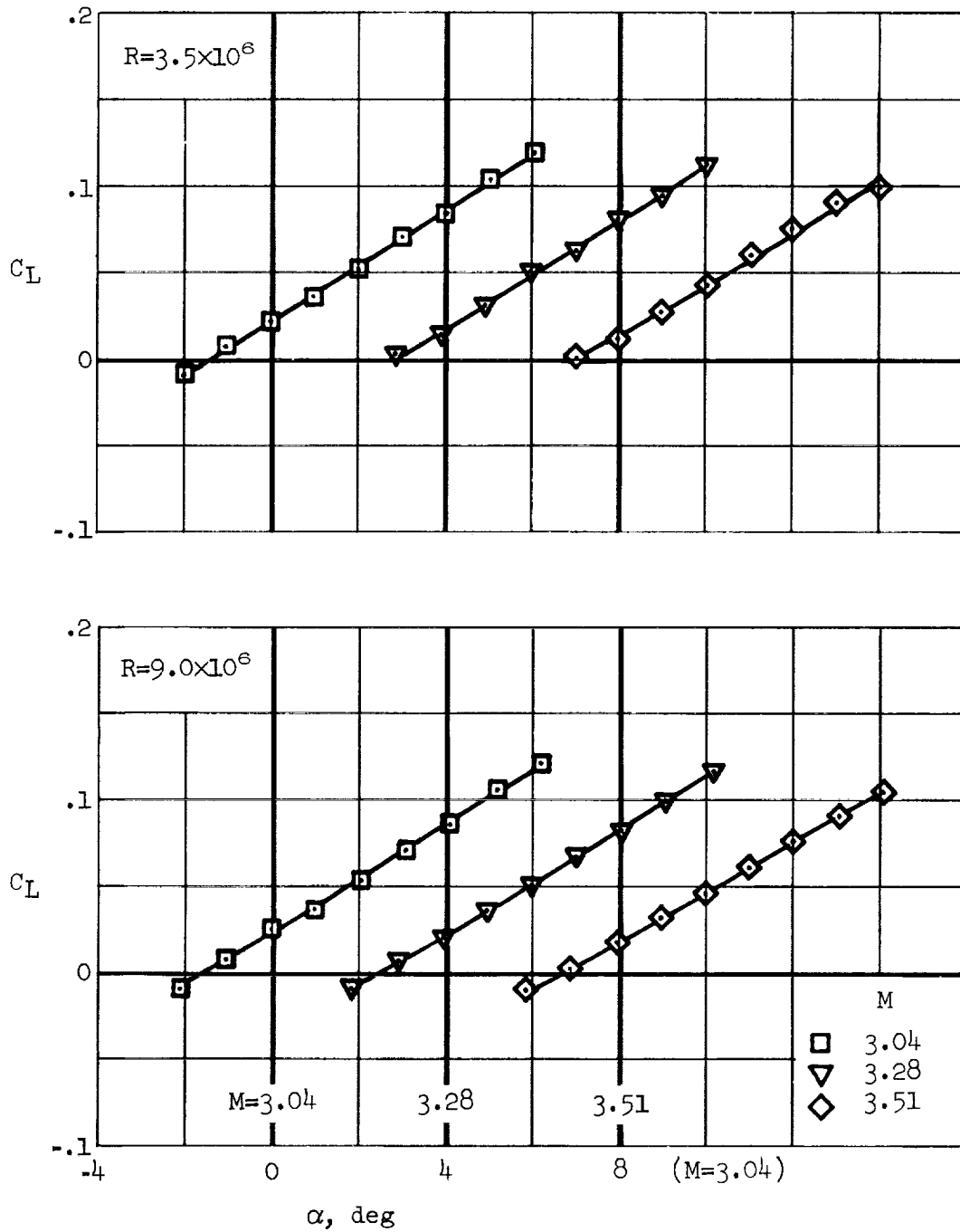
(a) C_L vs. α

Figure 5.- Lift, drag, pitching-moment, and lift-to-drag ratio
characteristics for the arrow wing with the unbent wing tips;
air ejected at wing leading edge; m=0.008 slugs/min.
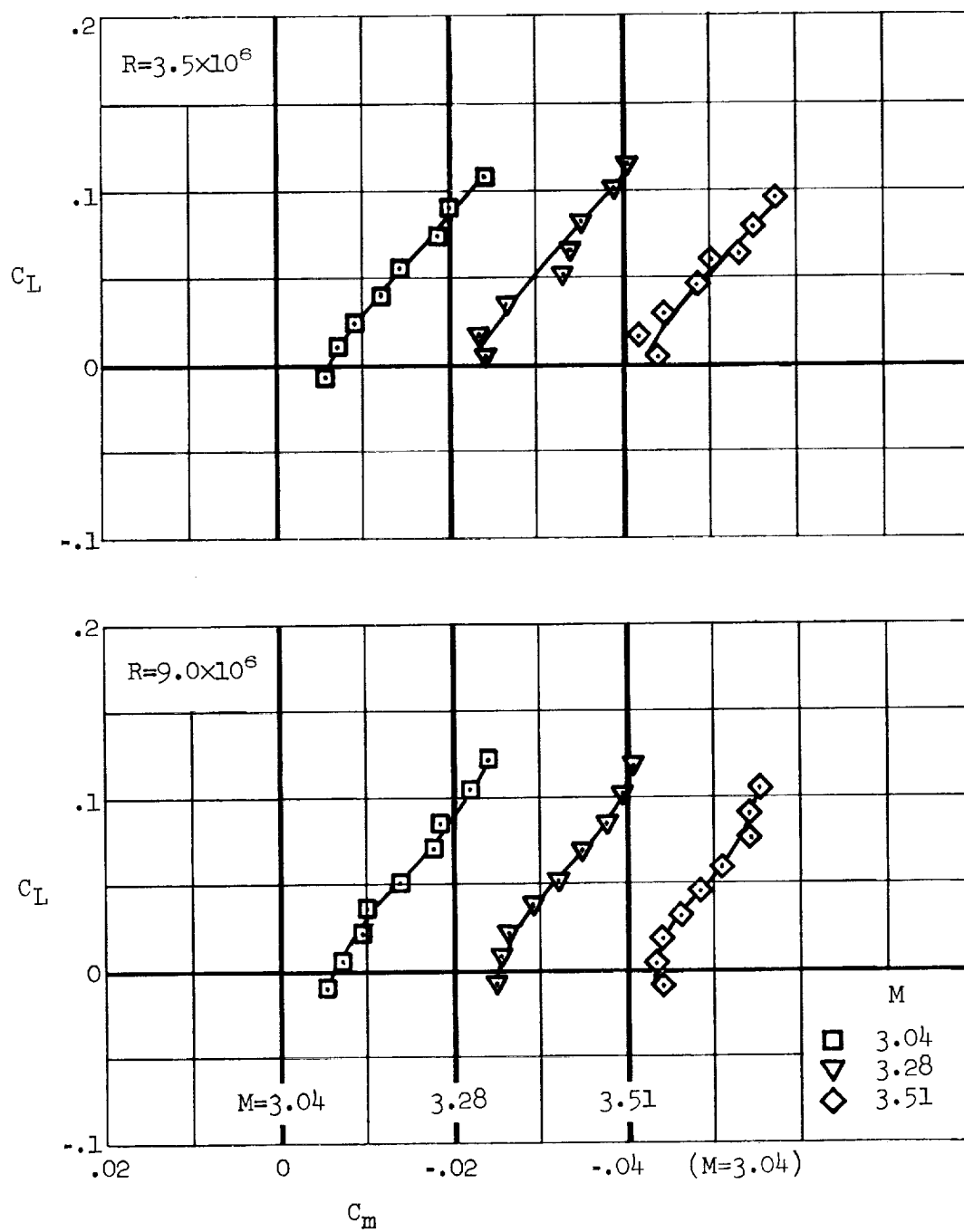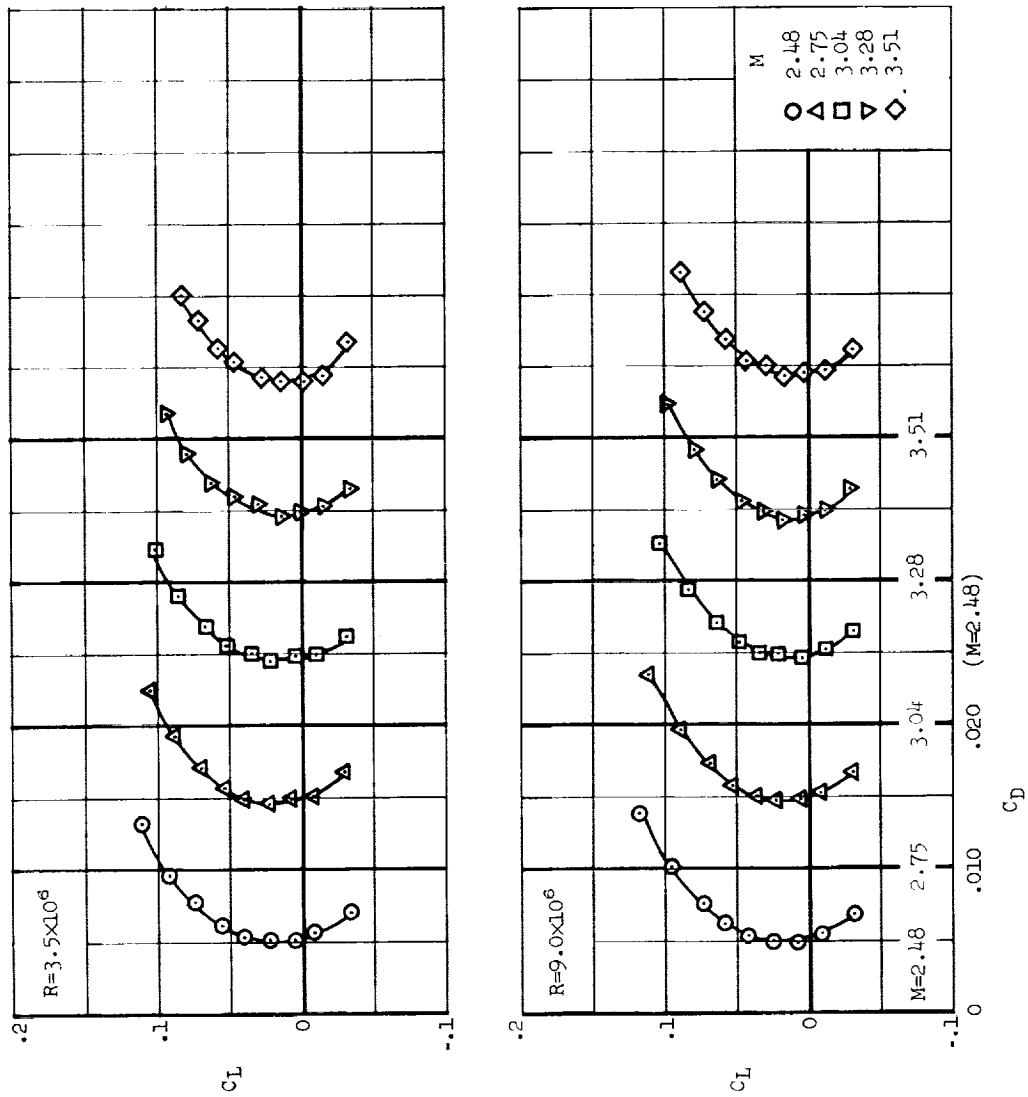
(b) C_L vs. C_m

Figure 5.- Continued.
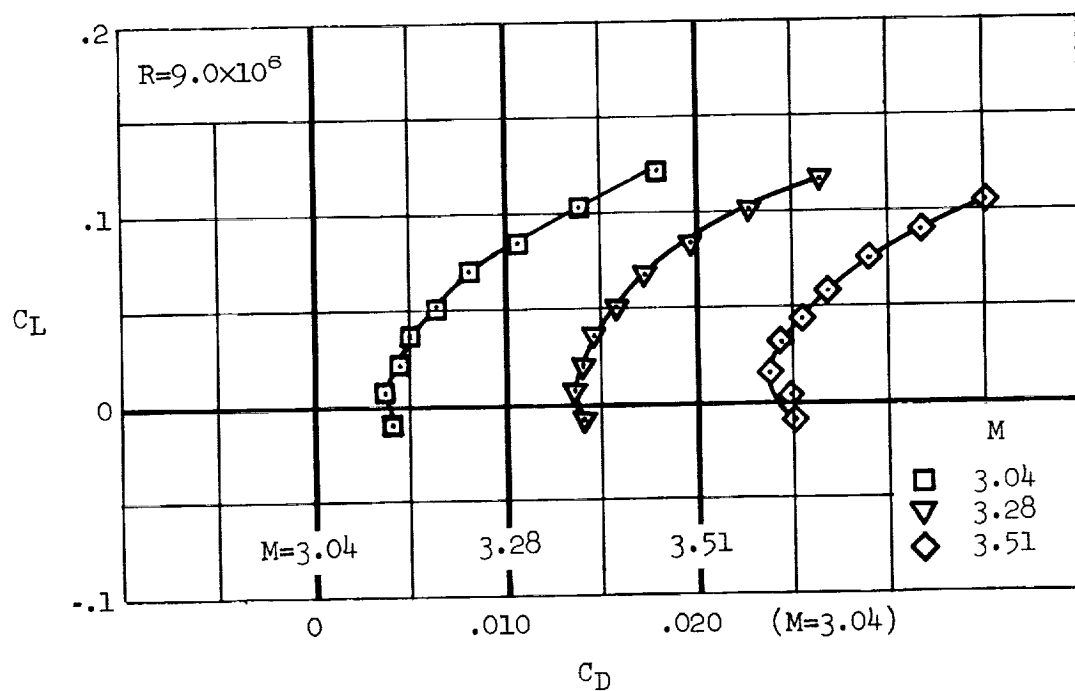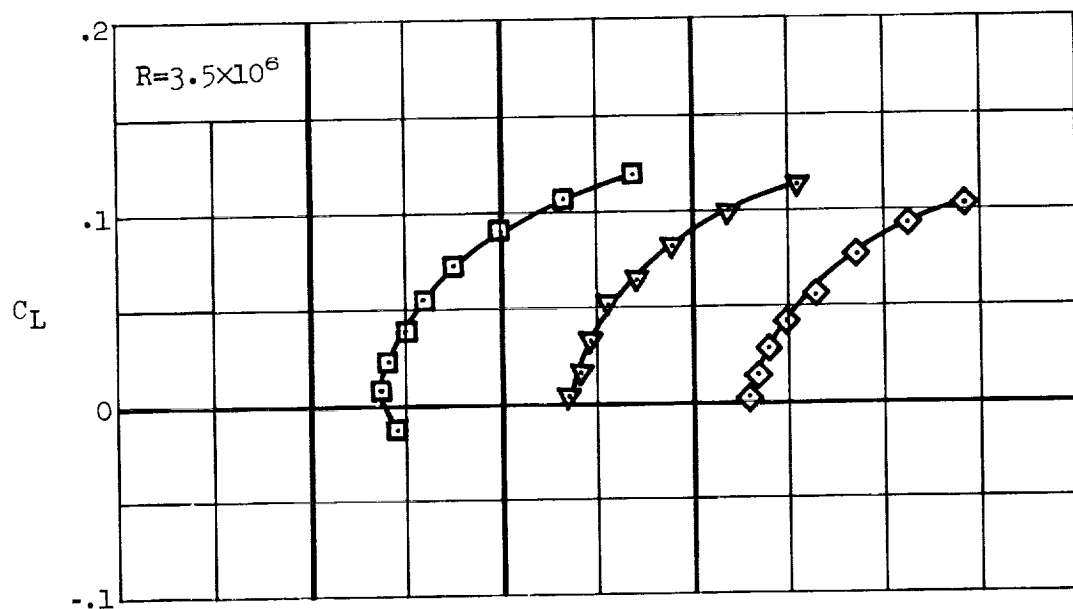
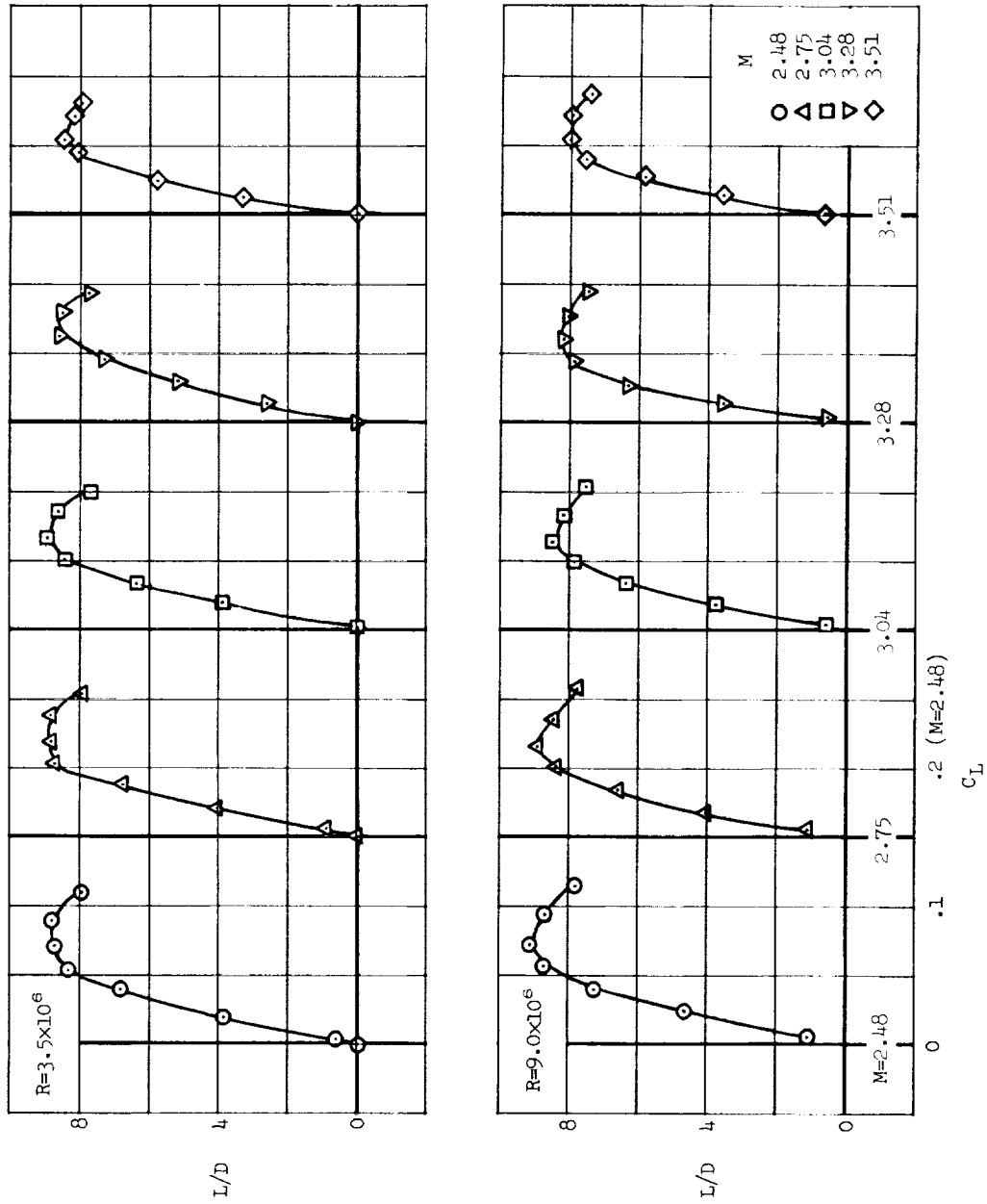(c) C_L vs. C_D

Figure 5.- Continued.
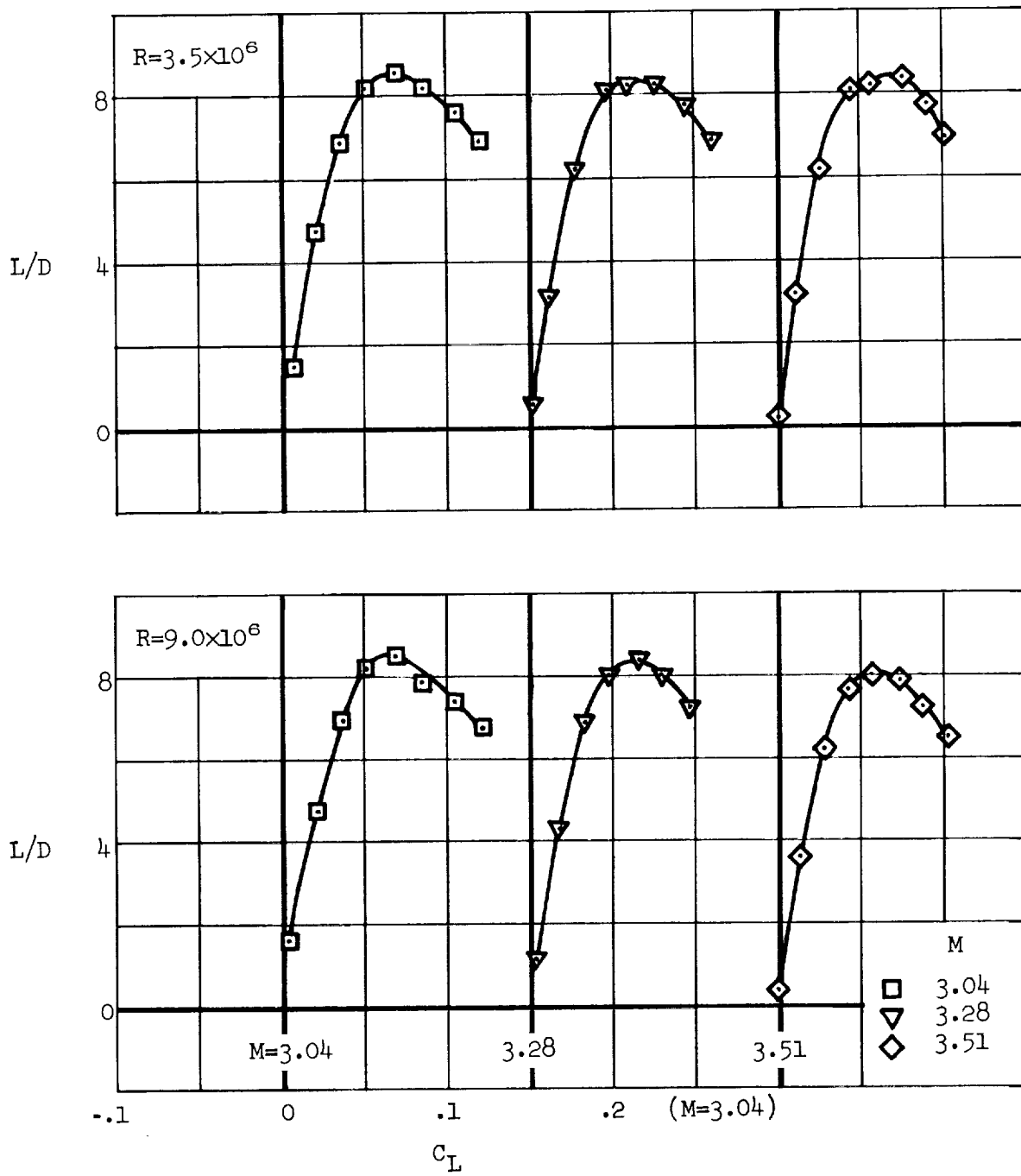
(d) L/D vs. C_L

Figure 5.- Concluded.
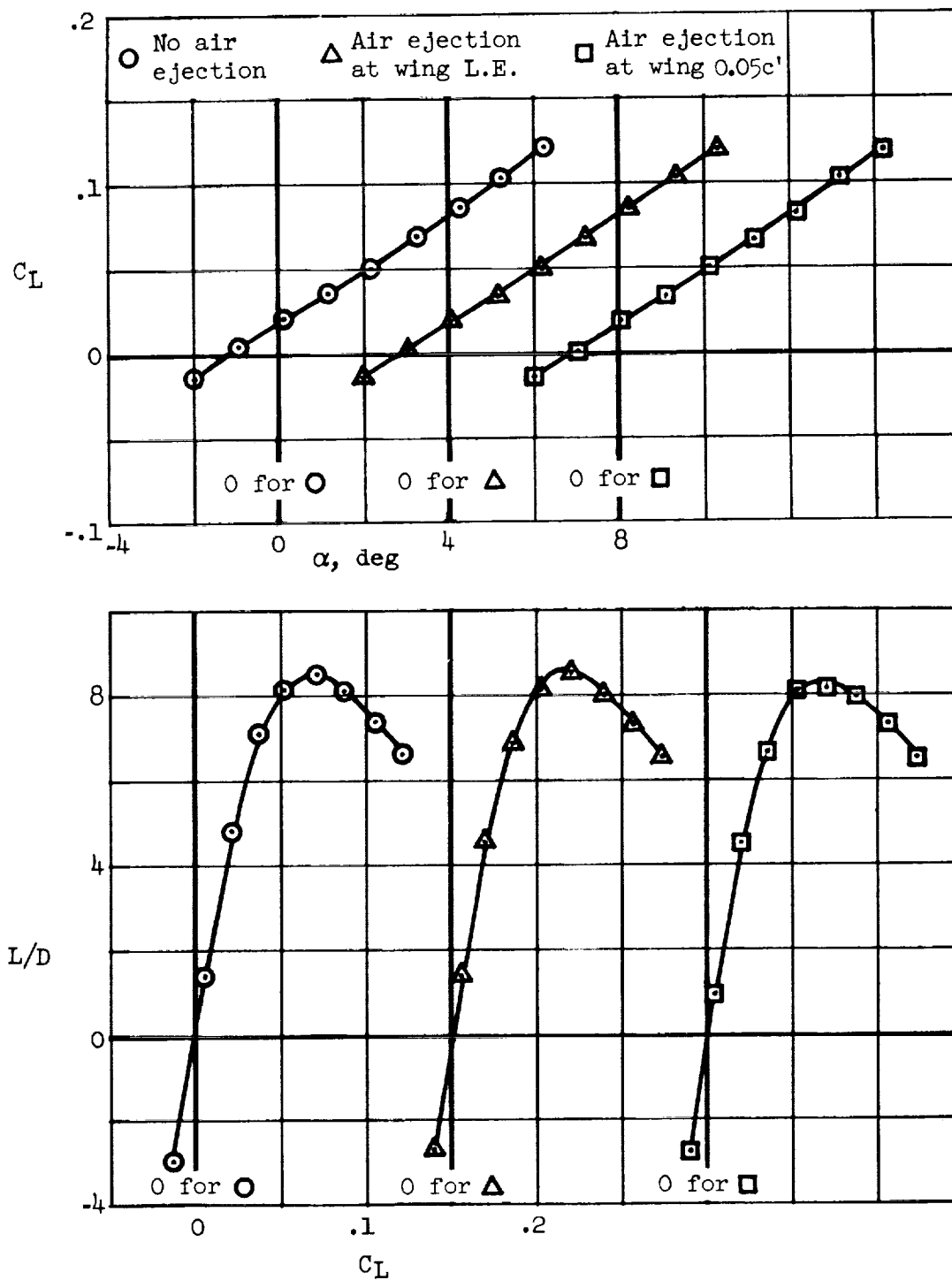
(a) C_L vs. α and L/D vs. C_L
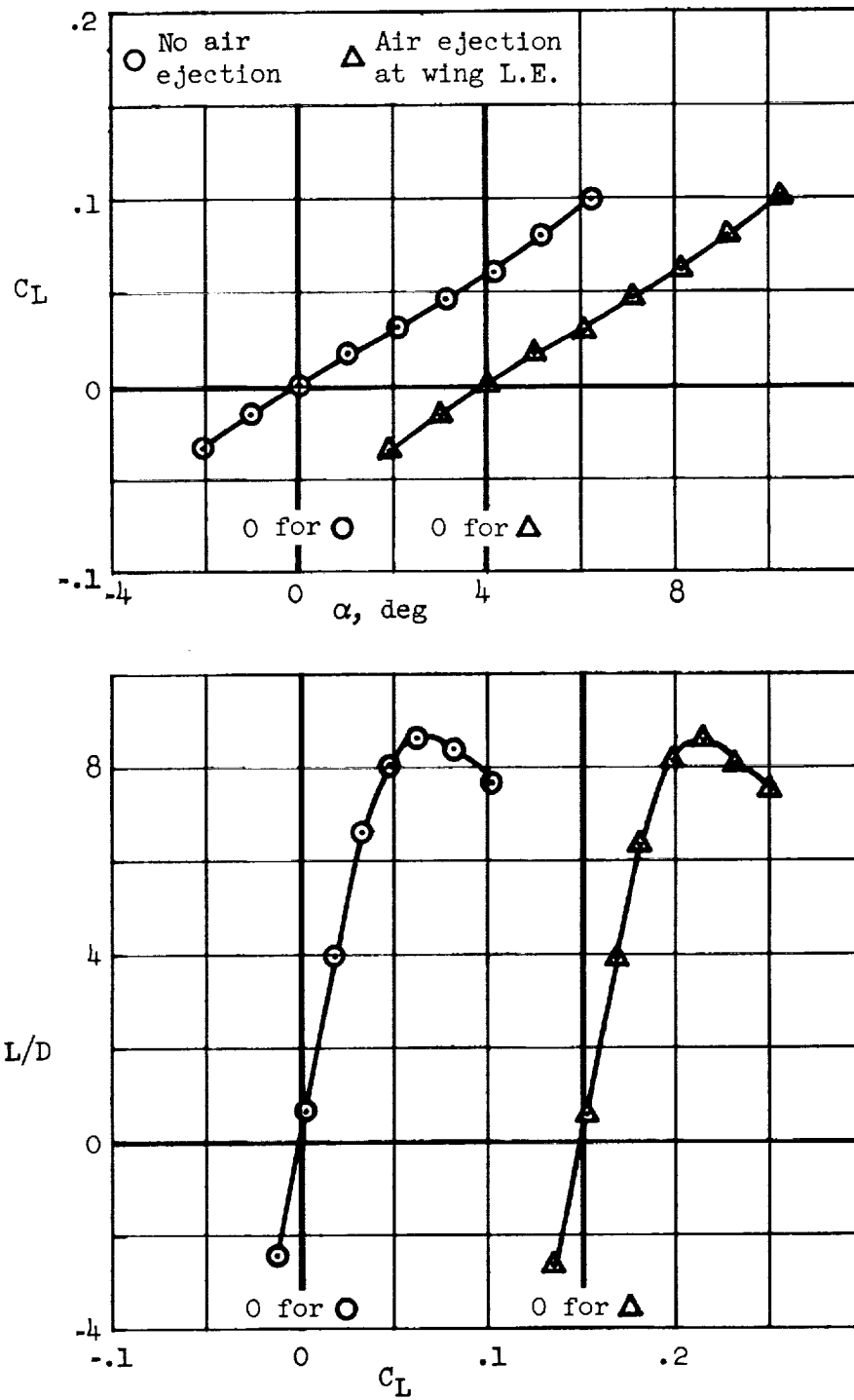
Figure 6.- Lift, drag, pitching-moment, and lift-to-drag ratio characteristics for the arrow wing with unbent wing tips; R=11.0x10^{6}, M=3.04.

29
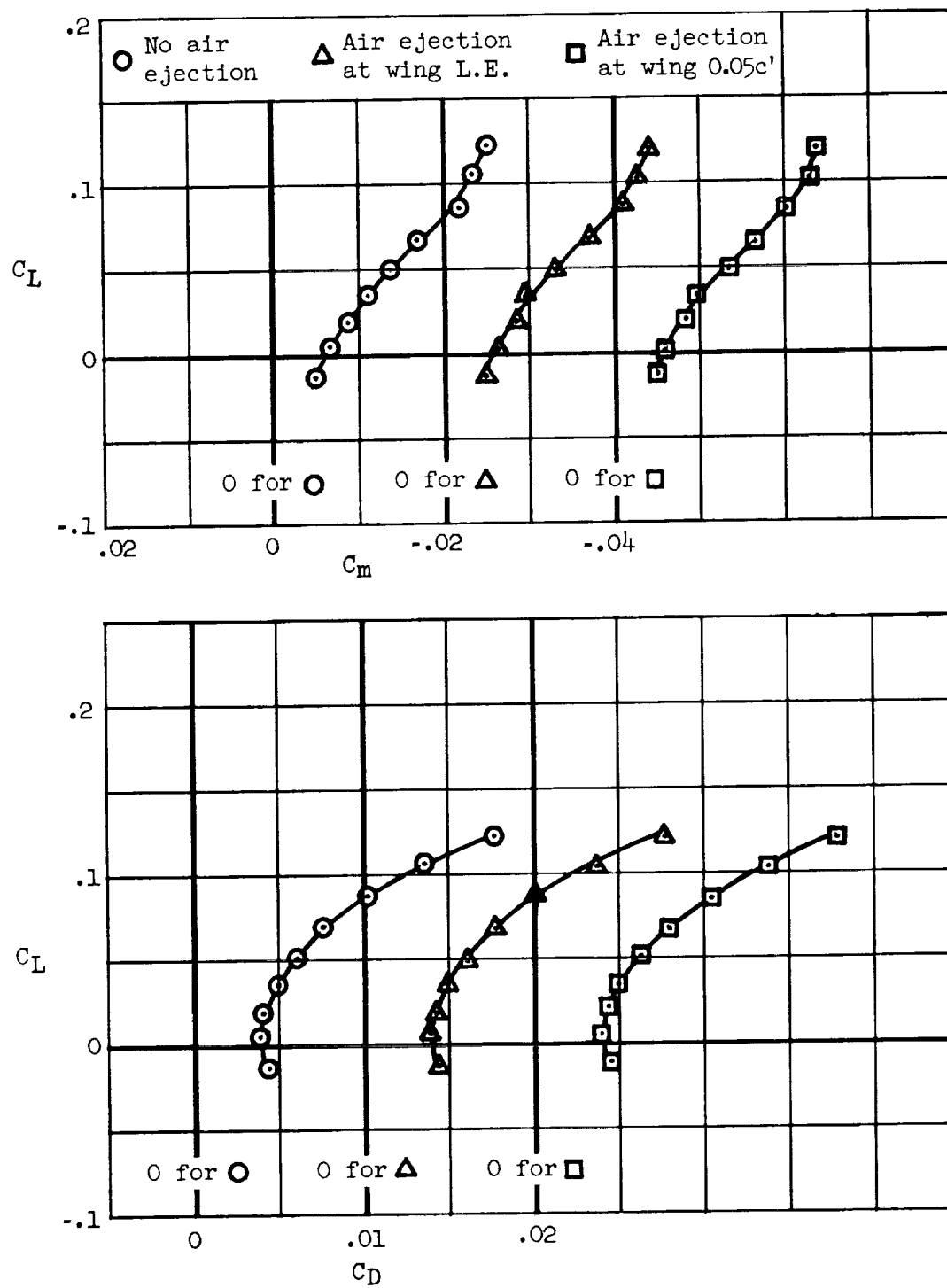
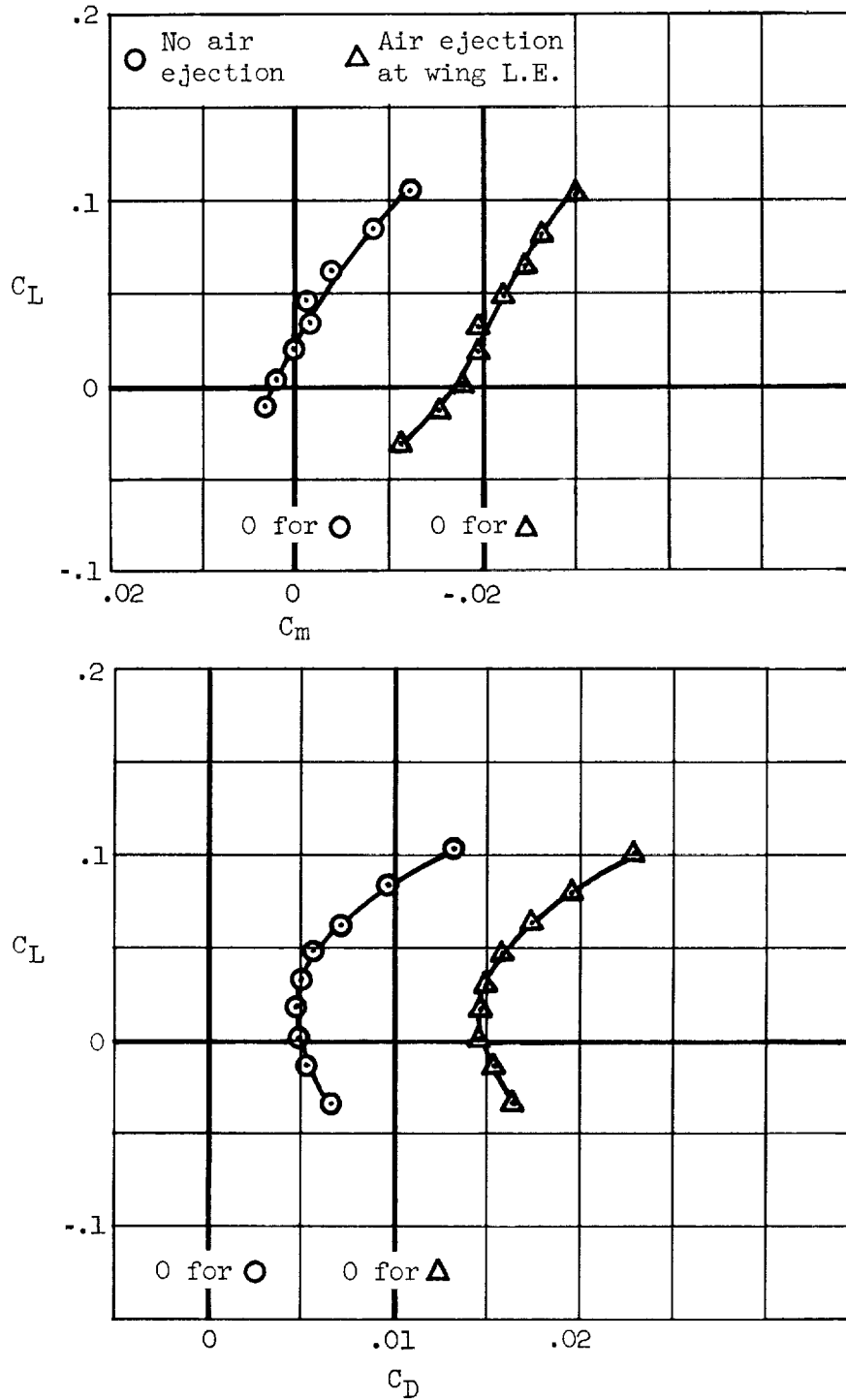(b) C_L vs. C_m and C_D

Figure 6.- Concluded.
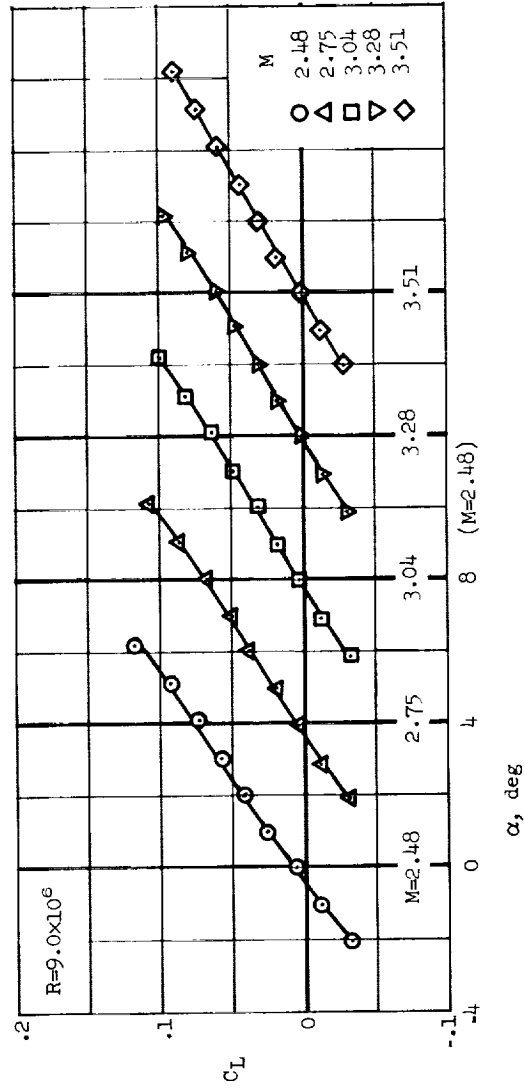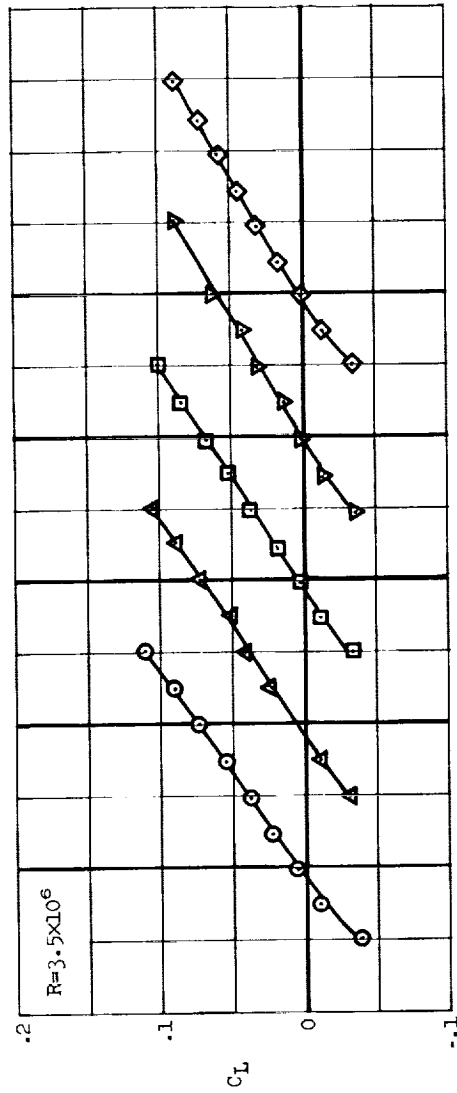
(a) C_L vs. α

Figure 7.- Lift, drag, pitching-moment, and lift-to-drag ratio characteristics for the arrow wing with the bent wing tips. No air ejection.
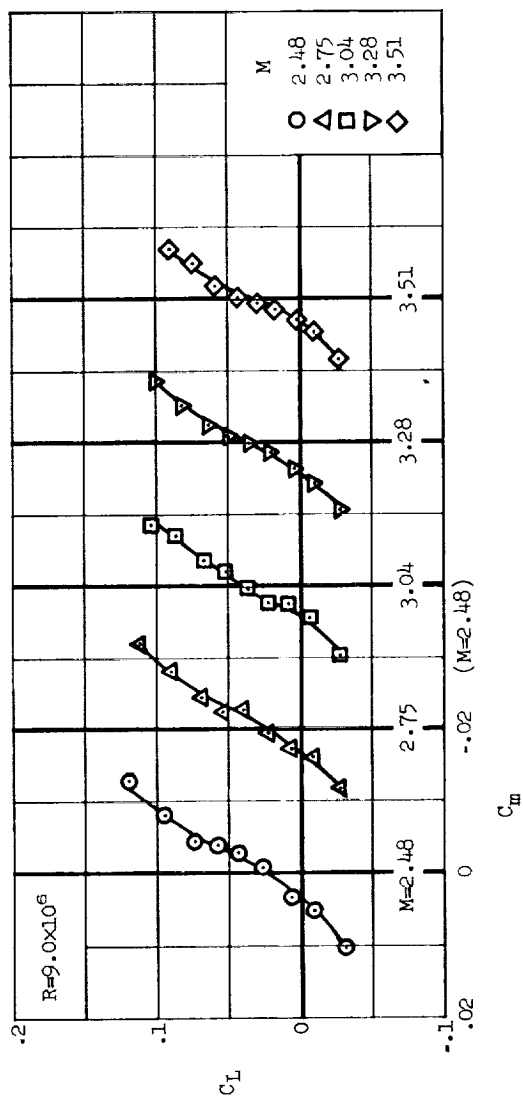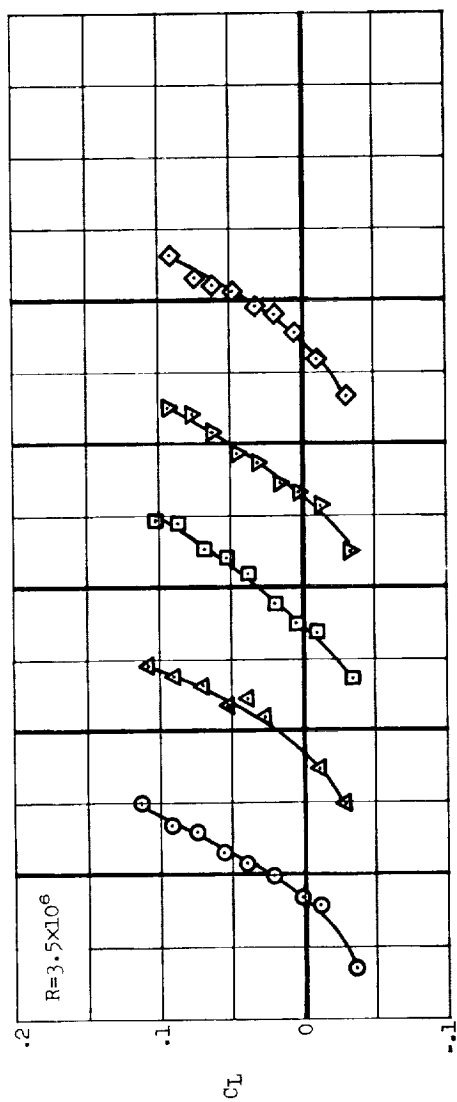
(b) C_L vs. C_m

Figure 7.- Continued.

(c) C_L vs. C_D

Figure 7.- Continued.

(d) L/D vs. C_L

Figure 7.- Concluded.

(a) C_L vs. α

Figure 8.- Lift, drag, pitching-moment, and lift-to-drag ratio characteristics for the arrow wing with the bent wing tips; air ejected at wing leading edge, m=0.009 slugs/min.
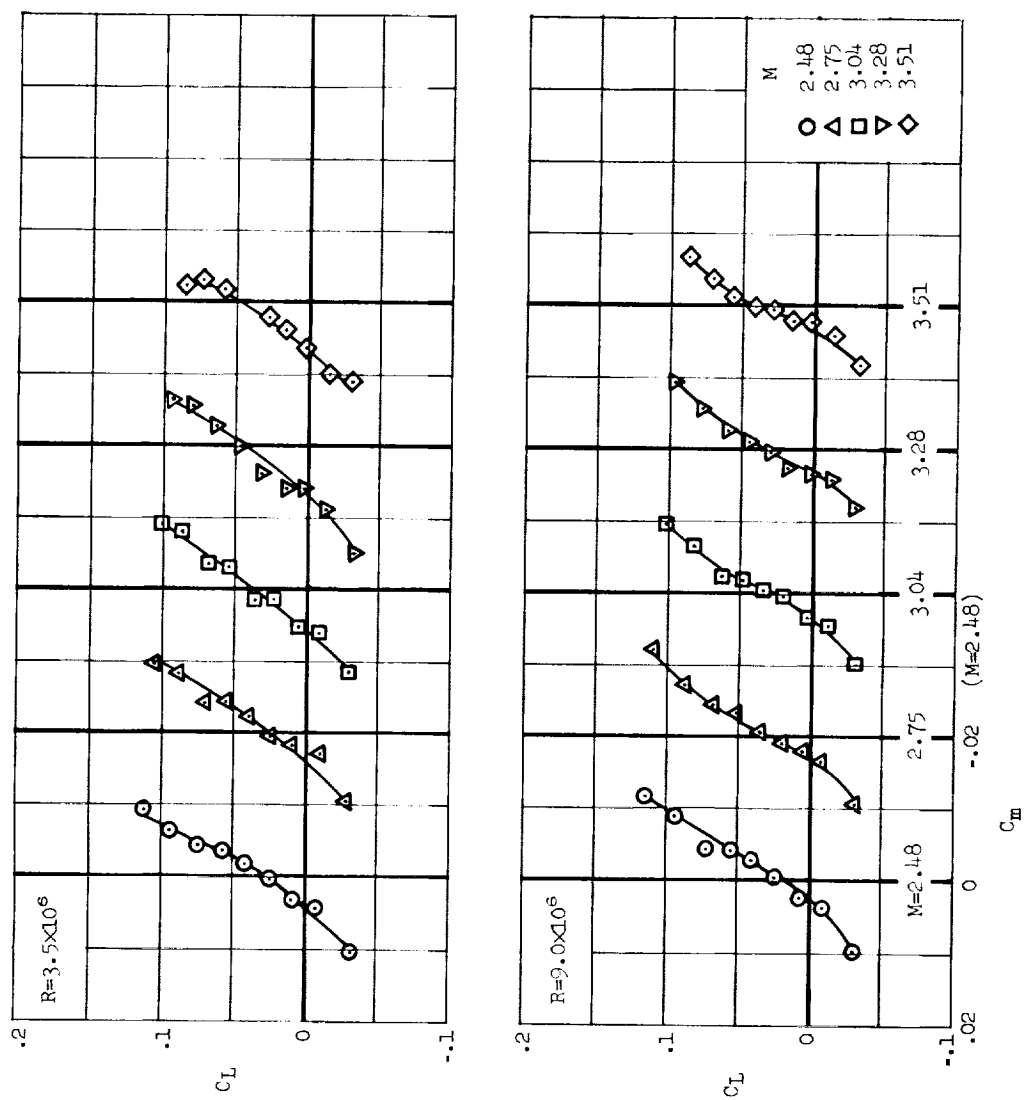
(b) C_L vs. C_m

Figure 8.- Continued.

(c) C_L vs. C_D

Figure 8.- Continued.

(d) L/D vs. C_L

Figure 8.- Concluded.

(a) C_L vs. α and L/D vs. C_L

Figure 9.- Lift, drag, pitching-moment, and lift-to-drag ratio characteristics for the arrow wing with bent wing tips; R=11.0x10⁶, M=3.04.

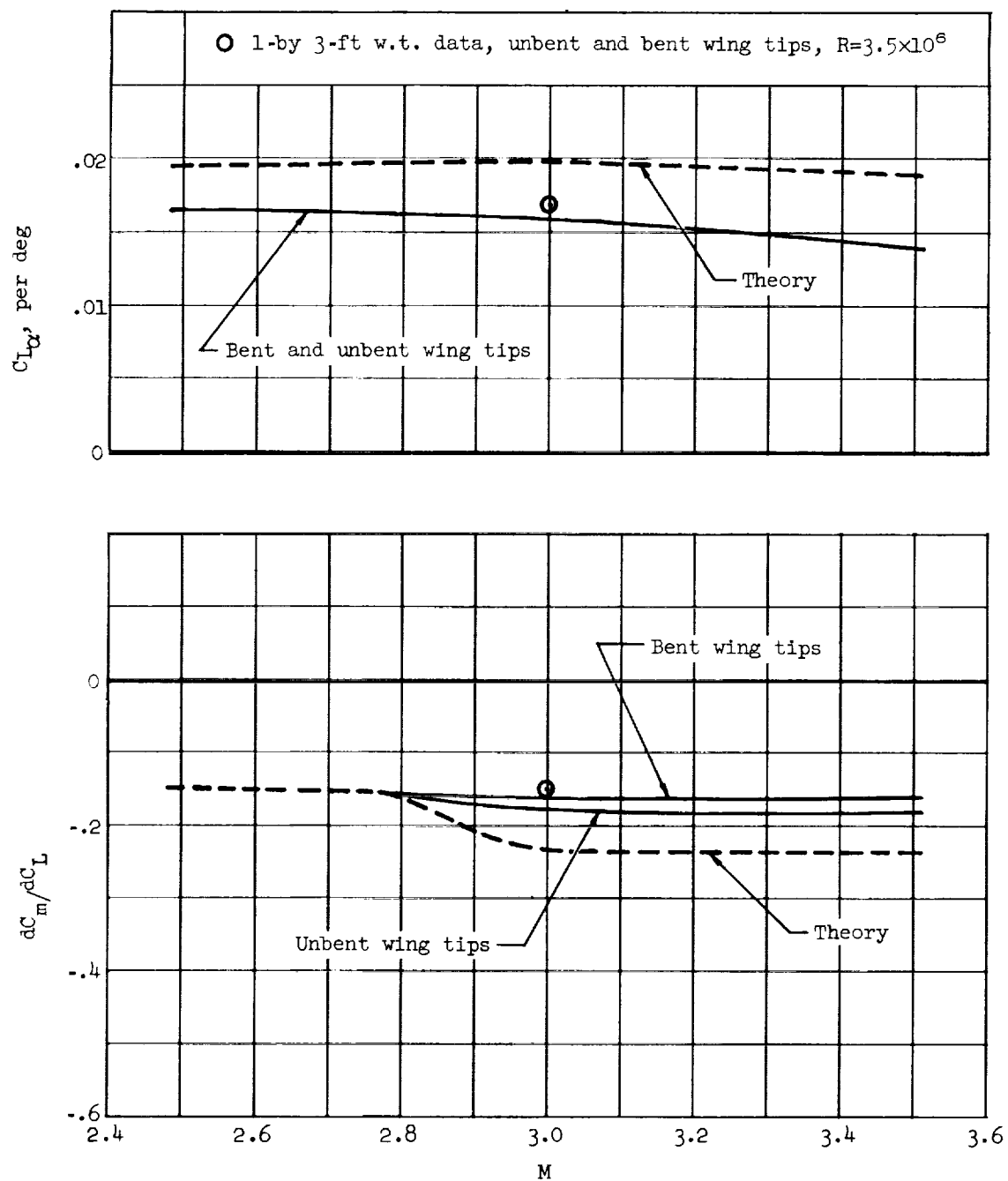(b) C_L vs. C_m and C_D

Figure 9.- Concluded.

(a) C_{L_α} and dC_m/dC_L vs. M

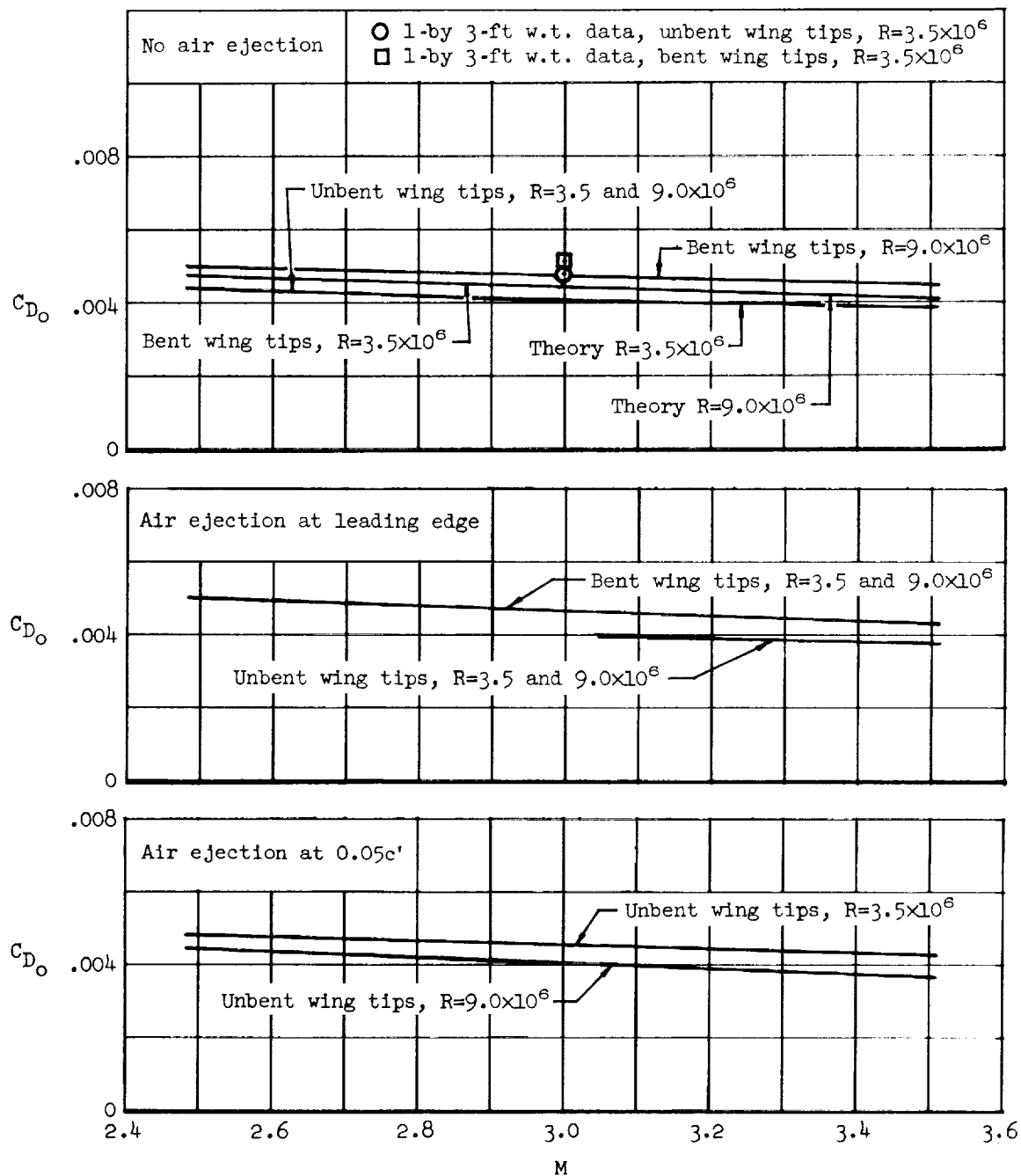Figure 10.- Summary of the aerodynamic characteristics as a function of Mach number.
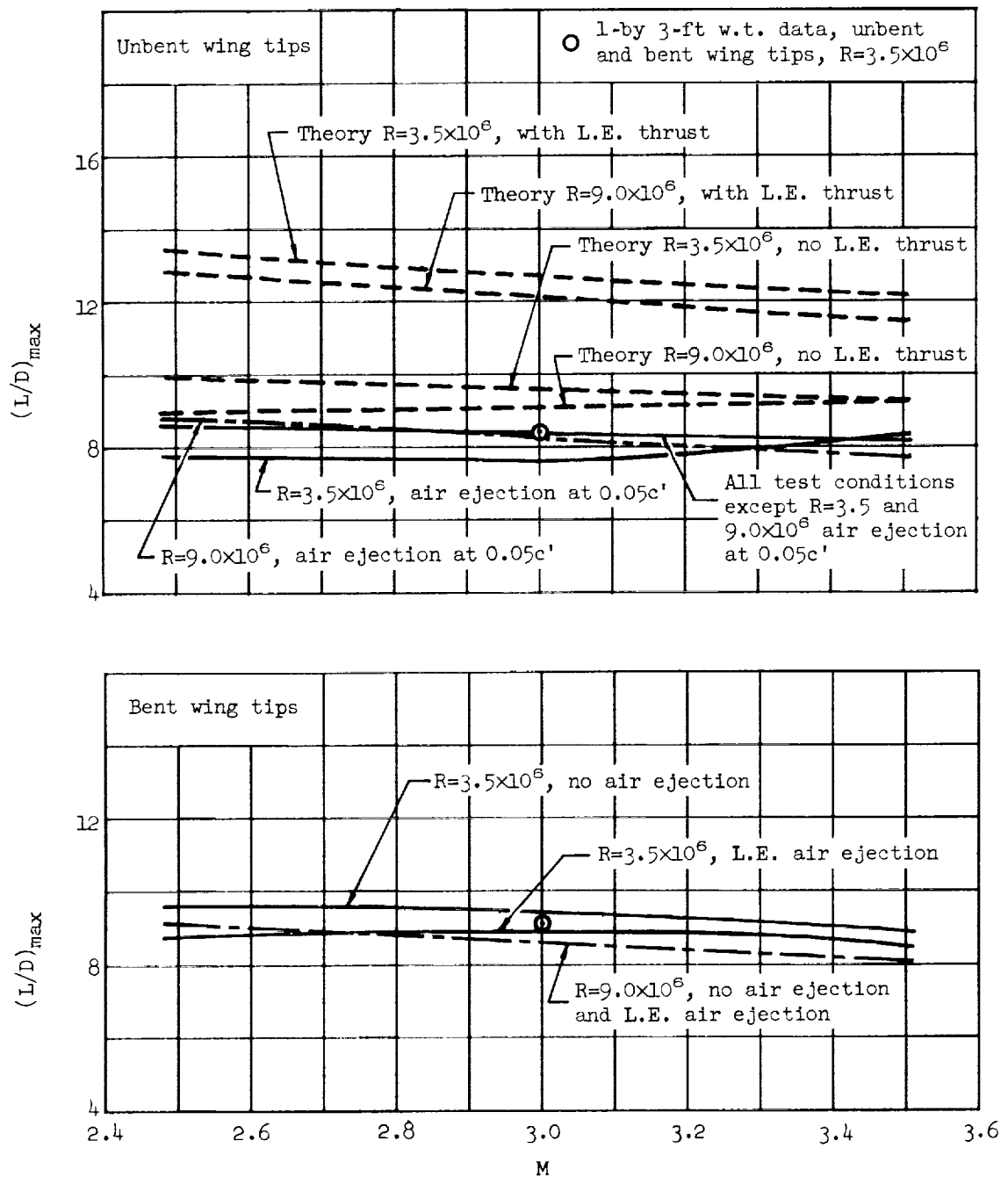
(b) C_{D_O} vs. M
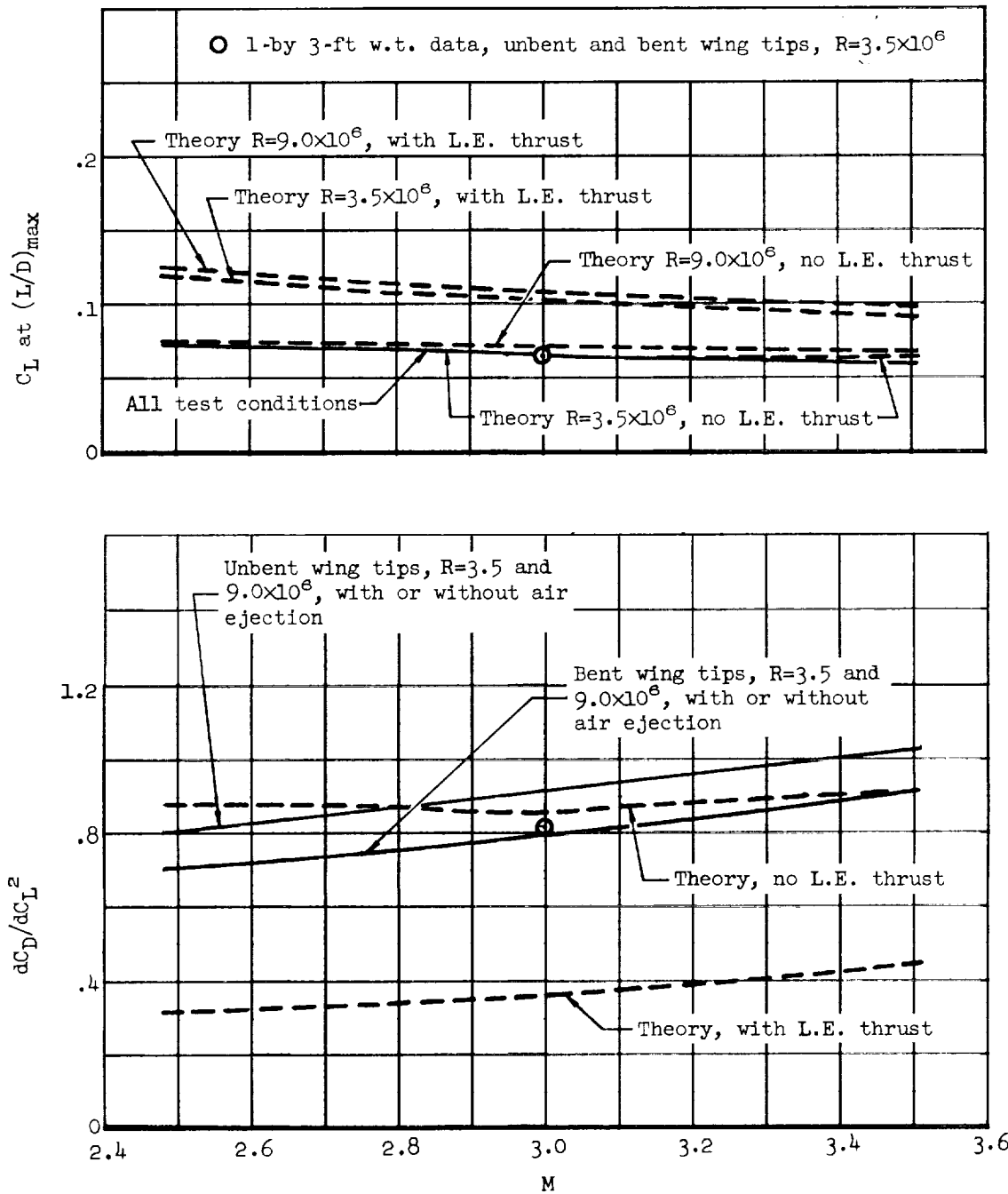
Figure 10.- Continued.

(c) $(L/D)_{max}$ vs. M

Figure 10.- Continued.

(d) C_L at $(L/D)_{max}$ and dC_D/dC_L^2 vs. M

Figure 10.- Concluded.